ARCHIVES OF ACOUSTICS
12, 1, 3–15 (1987)

THRESHOLDS OF PERCEPTION OF MIXED MODULATION*

EDWARD OZIMEK, ALEKSANDER SĘK

Institute of Acoustics, A. Mickiewicz University in Poznań
(60–769 Poznań, ul. Matejki 48/49)

This paper is concerned with the determination of perception thresholds of mixed modulation (*MM*) for chosen physical parameters of a signal. Besides a tonal modulating signal, also an irregular modulating signal in the form of a very narrow noise band with a definite mid-band frequency was applied in the course of research.

It was stated that the perception of modulated signals is governed by two mechanisms: the time mechanism and the spectral mechanism, which do not depend on the type of modulation. These mechanisms become evident at definite values of the modulation frequency, which, as we know, conditions the rate of amplitude and frequency changes of the modulated signal.

We have to do with the time mechanism at slow changes of physical parameters of this signal (low modulating frequency). Whereas, when the changes of these parameters are quick (high modulating frequency) the spectral mechanism takes place.

The hypothesis concerning the existance of such perception mechanisms was confirmed by obtained experimental results.

1. Introduction

The problem of perception of sound amplitude and frequency changes has been widely discussed in literature — from the point of view of psychoacoustic investigations [1, 3, 5, 6, 10–12] and neurophysiologic studies [8, 9]. Two main hypothesis' concerning the perception of amplitude-frequency changes of a signal can be distinguished. One of them was presented by ZWICKER [11] and MAIWALD [6, 7]. It assumes that amplitude and frequency changes are registered by one and the same perception mechanism. Whereas, the second hypothesis presented by Coninx [1], assumes that two independent perception mechanisms of these changes exist, i.e. a separate perception mechanism of amplitude changes and separate perception mechanism of frequency changes.

* Research was performed within the framework of problem MR.I.24.IX.

A solution to this problem was sought in various experiments, which concerned thresholds of amplitude and frequency modulation perception [10, 12], difference limens of loudness and pitch [3], monaural phase perception [4], etc. These experiments have contributed significantly to a fuller description of the discussed problem. However, they did not confirm the justness of one out of the two presented hypothesis'.

An unconventional approach to the mentioned above problem was presented in papers [1, 2, 5–7, 11], which concern the perception of simultaneous amplitude and frequency changes with modulation (so-called mixed modulation, *MM*). The perception of amplitude and frequency changes in the case of the first hypothesis, which accepts the existance of a single, common mechanism, should proceed in a similar manner.

This means that the perception of frequency changes at mixed modulation should depend on coexisting amplitude changes. Whereas, in the case of the second hypothesis, which accepts the existance of two independent mechanisms, the perception of amplitude changes in the conditions of mixed modulation should be independent from coexisting frequency changes.

ZWICKER'S paper [11] is on of the first, which postulates the existance of one perception mechanism of amplitude and frequency changes of a singal. It analyses the sensation created by amplitude (*AM*), frequency (*FM*) and mixed (*MM*) modulation of an octave noise band (1–2 kHz), partially masked by a noise contained in band 2–10.5 kHz. It results from this paper that amplitude modulated signals can be evaluated as equal to frequency modulated signals, if adequate modulation indices (i.e. m and β) strictly satisfy definite relations. Investigations on the possibility of equalizing senstations created by mixed modulation and frequency modulation have proved that for a *MM* signal two effects, dependent on the phase difference between signals which modulate amplitude and frequency, can occur. Consistant phases of these signals cause a "deepening" (addition) of modulation effects, expressed by an increased deviation of the *FM* signal. As for opposite phases of these signals, the intensification of the modulation effect is observed only at lower frequencies ($f_m < 100$ Hz) and for values of the amplitude modulation factor exceeding 20–30%, while for the modulating frequency equal to $f_m = 50$ Hz and for $m \leqslant 20\%$, the modulation effect is attenuated.

MAIWALD'S paper [6] deals with a similar problem. Instead of a modulated noise octave, as in paper [11], a simple tone with amplitude and frequency modulated at the same time was applied. This research has led to results similar to those obtained in paper [11]. It should be noticed that mentioned above papers [6, 11] deal with relatively slow amplitude and frequency changes of the signal (ZWICKER — $f_m = 3$ and 10 Hz; MAIWALD — $f_m = 4$ Hz), and high values of deviation and amplitude modulation factor in comparison with threshold values.

Results of papers presented above have contributed to the formation of a functional perception model of modulated signals. According to this model, one mechanism governs the perception process of small amplitude and frequency

changes. On the basis of this model, supplemented with MAIWALD'S more recent studies [7], the perception threshold of amplitude modulation can be calculated, as well as loudness difference limens, if the spectrum of the acoustic signal is known.

The problem of perception of *MM* signals and *MM* signals partially masked with a noise band, for consistant and opposite phases of amplitude and frequency modulating signals, has been analysed in CONINX'S paper [1]. These studies have led to the normalization of curves of just noticeable amplitude and frequency modulation in relation to threshold values. The cooperation of both types of modulation can be evaluated from these curves. Coninx gives the relationship between the threshold of amplitude modulation and coexisting frequency modulation at the absence of other signals for only one case. On the basis of this relationship it can be stated that a case of consistant phases of modulating signals, at definite experimental conditions (i.e. carrier frequency 8 kHz and modulating frequency 5 Hz), the coexistance of two types of modulation causes the "summation" (in the sense of mutual aid) of sensations created by both types of modulation. In the case of opposite phases between modulating signals, the cooperation of these types of modulation do not influence the values of thresholds so significantly. Values of thresholds are approximately independent from the coexisting modulation with sub-threshold value. A final conclusion can be drawn from research performed by CONINX — two independent perception mechanism of amplitude and frequency changes exist. According to CONINX, the cooperation between amplitude and frequency changes, which was proved on the basis of asymmetric shapes of curves of just noticeable modulations, can be explained not on the basis of one perception mechanism of amplitude and frequency changes, but on the basis of a mutual influence of amplitude on the pitch, and of frequency on the loudness of a signal. This problem has been also considered in detail in paper [3]. In another paper [2] CONINX tried to explain differences in the perception of *MM* signals with consistent and opposite phases between modulating signals, by converting amplitude and frequency changes into loudness and pitch changes, respectively.

Also the paper of HARTMANN and HNATH [5] is an important work in this domain. It deals with the perception of modulated signals; *AM*, *FM* and *MM*, and includes the masking effect. This paper was aimed at the determination of the individual components of a signal spectrum on values of the threshold of modulation perception. The dependence of the threshold of mixed modulation perception on the quotient of frequency and amplitude modulation indices for a case of consistent and opposite phases between signals modulating amplitude and frequency is especially important in this work.

This paper has led to the extension of the perception model of modulated signals, which was developed by GOLDSTEIN [4], and to the determination of its two boundary cases. These are: non-summation model, according to which the modulation is percepted on the basis of the dominating spectrum component; and the envelope fluctuation model, according to which the modulation takes place due to the perception of fluctuations of physical parameters of a modulated signal. On

the basis of the discovered relationship between adequate modulation indices on the threshold of mixed modulation perception, HARTMANN and HNATH could support ZWICKER'S hypothesis [12], which assumes the existance of one mechanism responsible for the perception of amplitude and frequency modulation.

2. Time and spectral structure of *MM* signals

Let us consider a tonal signal with angular frequency ω_o in the following form

$$a(t) = A(t)\cos\omega_0 t, \tag{1}$$

with amplitude and frequency modulated by another tonal signal

$$b(t) = B\cos\omega_m t. \tag{2}$$

The time structure of this signal can be written as

$$a(t) = A_0[1+m\cos(\omega_m t+\varphi)]\cos[\omega_0 t+\beta\sin(\omega_m t+\psi)] \tag{3}$$

where m and β denote amplitude and frequency modulation indices, respectively, and $\varphi-\psi$ is the phase shift between signals, which modulate amplitude and frequency. Making use of a simple trigonometric transformation and assuming that $m, \beta \ll 1$ it can be easily proved that

$$\begin{aligned} a(t) \approx{}& A_0\cos\omega_0 t+(A_0/2)(m\cos\varphi-\beta\cos\psi)\cos(\omega_0-\omega_m)t \\ &+(A_0/2)(m\cos\varphi+\beta\cos\psi)\cos(\omega_0+\omega_m)t \\ &+(A_0/2)(m\sin\varphi-\beta\sin\psi)\sin(\omega_0-\omega_m)t \\ &-(A_0/2)(m\sin\varphi+\beta\sin\psi)\sin(\omega_0+\omega_m)t. \end{aligned} \tag{4}$$

As it results from equation (4), the spectrum of an amplitude and frequency modulated signal consists of three fundamental components — the central one represents the carrier signal, while the sidebands are results of modulation. It should be noticed that amplitude values of sidebands depend on the mutual phase shift of signals, which modulate amplitude and frequency. When this shift equals $\varphi = \psi = 0$, then amplitude of the bands are proportional to $m-\beta$ for the lower and to $m+\beta$ for the higher band (Fig. 1).

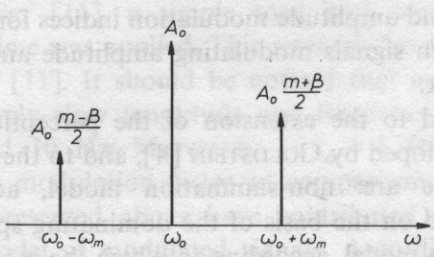

Fig. 1. Spectrum of signal simultanously amplitude and frequency modulated by a sinusoidal signal (see relationship (4)

The determination of the spectrum of a tone with amplitude and frequency modulated by a random signal is a more complicated problem than in the case of a tone modulated by a sinusoidal signal. The random modulating signal was accepted as the result of a stationary ergodic process with a normal distribution, in order to determine the spectrum of such a tone. Then its autocorrelation function, *rms* value and correlation function for the modulated signal could be derived. Additionally, the power spectral density of the modulated signal could be determined on the basis of the WIENER–CHIŃCZYN theorem.

This new method of determination of modulated signals is inconvenient in practice, because (in a case of correlated signals which modulate amplitude and frequency) the probability distribution of the product of the random signal and its integral has to be found. Moreover, this method does not give a direct measure of modulation, which has to be defined for measuring purposes.

Therefore, in this paper certain simplifying assumptions concerning the random modulating signal were made in order to determine the spectrum of a tone modulated by a random signal. Namely, the modulating signal (in this case a very narrow noise band) can be approximated by a tone with its frequency equal to the mid-band frequency and the amplitude equal to the rms of the noise band. And so,

$$n(t) = \sqrt{\sigma^2}\cos\omega_m t,$$

where σ is the variance of the noise band. When an assumption is made, that the phase shift $\varphi - \psi$ between the amplitude and frequency modulating signal is equal to zero, then the time and spectral form of the modulated signal can be noted in an analogic manner as in the case of a signal modulated by a tone, i.e.

$$a(t) = A_0(1 + m_{ef}\cos\omega_m t)\cos(\omega_0 t + \beta_{ef}\sin\omega_m t) \tag{5}$$

and

$$a(t) \approx A_0\cos\omega_0 t + (A_0/2)(m_{ef} - \beta_{ef})\cos(\omega_0 - \omega_m)t + (A_0/2)(m_{ef} + \beta_{ef})\cos(\omega_0 + \omega_m)t. \tag{6}$$

Quantities

$$m_{ef} = (\sqrt{\sigma^2}/A_0)k; \quad \beta_{ef} = \Delta\omega_{ef}/\omega_m = (\sqrt{\sigma^2}/A_0)k' \tag{7}$$

denote the *rms* index of amplitude modulation factor and the *rms* index of frequency modulation, respectively. They are the measures of modulation. It results from equation (6) that the spectrum of a tone with the amplitude and frequency modulated by a noise band is similar to the spectrum of a tone modulated by a sinusoidal signal, however, sidebands appear instead of spectral components. An identical result can be achieved under an assumption that the modulating noise band consists of a finite amount of components with adequate amplitude and frequencies, which are within this band. The obtained above form of a spectrum of a tone amplitude and frequency modulated by a random signal has been confirmed by results of an experimental analysis of modulated signals, which were audio monitored during the course of investigations.

3. Aim of research

As it results from paragraph 1, the problem of mixed modulation has been undertaken in many research contexts. First works on mixed modulation concerned the evaluation of signals modulated with the application of such values of modulation indices, which considerably exceeded thresholds of their perception. Only CONINX (carrier frequency 8 kHz, modulating frequency 5 Hz) [1] and HARTMANN (carrier frequency 1 kHz and modulating frequency 25 Hz) have determined thresholds of perception of mixed modulation with a varying percentage share of amplitude and frequency modulation. Signals used in papers [1, 5] are relatively simple, regular sinusoidal signals, which differ from occuring in practice signals, which determine amplitude and frequency changes (e.g. in speech or music).

Research performed here was aimed at the determination of thresholds of perception of changes occurring in an amplitude and frequency modulated (*MM*) signal in two cases. In the first case a regular signal (sinusoidal) was the modulating signal, while in the second case — an irregular signal (random), which was applied in such investigations for the first time. The application of a random modulating signal allowed a closer approximation of reality (i.e. sounds of speech and music, which are characterized by irregular changes of amplitude and frequency) by experimental conditions. Moreover, a comparison could be done between changes of thresholds of perception in both cases, i.e. regular and irregular changes of physical parameters of an MM signal.

4. Apparatus and research methods

A generator with the amplitude and frequency of the output signal controlled by external voltage, was the main element of the apparatus applied in the determination of thresholds of perception of simultaneous amplitude and frequency changes of a modulated signal. In dependence on the type of experiment, either a tone generator or a white noise generator with a filtering system were used as the source of voltage.

Simultaneous amplitude and frequency changes were archieved as a result of mixed modulation (*MM*) of a tone by a sinusoidal or random signal. Regular or irregular changes of physical parameters of the modulated signal were obtained. Measurements of threshold values for a case of a tone-tone modulation were performed for a signal with frequency equal to: 4, 64, 400 Hz. These values of modulation frequency to a certain extent represent three characteristic regions of perception of modulated signals. Namely: the "follow up" region, where the organ of hearing keeps up with the observation of loudness maxima and minima, and the pitch of a signal; the roughness region, where changes of physical parameters occur so quickly that the ear is not able to register them and sufficiently slowly for sidebands of the spectrum to belong to the same critical band; region of separation of sidebands, where sidebands of the spectrum are outside the critical band, which corresponds to the carrier signal.

Measurements for a case of an irregular modulating signal were performed for a signal with the carrier frequency equal to 1000 Hz and for three bands of modulating noise with the width of 1.5% mid-band frequencies equal to 4, 64, 400 Hz.

In the course of all experiments the signal was presented monaurally through *SN* 60 earphone. The intensity level of a signal was constant and equal to 75 dB, and the phase shift between signals modulating amplitude and frequency was equal to zero.

Measurements were carried out on the basis of a modified tuning method. According to this method, the listener with the application of a special controller set such a value of amplitude modulation factor or its deviation, which was evaluated as threshold. This was done in two series: ascending, from very small subthreshold changes of m or β values to just noticeable values; and descending, from very high supra threshold values of m or β, at which the modulation was clearly audible to the moment at which the signal did not change at all, according to the listener. Data obtained in ten ascending tests and ten descending tests were statistically tested with the test of goodness of fit, test of rank sum, F-Snedecor test at the significance level of $\alpha = 0.05$, in order to determine whether results from both series are from one population. Positive results of these tests have supported this hypothesis.

Two listeners with audiologically normal hearing participated in the experiment.

5. Results of measurements and their analysis

Thresholds of perception of amplitude modulation and frequency modulation were determined seperately in the first part of investigations in order to compare them with data from literature and to verify applied methods. Experiments were performed for a regular and irregular modulating signal. Obtained results are presented in Figs. 2a and 2b — for listener *EO* and *AS*, respectively. These figures also show experimental results achieved by ZWICKER [12] for comparative reasons. Figs. 2a, b prove obtained results to be quantitatively and qualitatively consistant with data from literature.

Thresholds of perception of amplitude and frequency modulation differ strongly at low modulating frequencies ($f_{mod} \leqslant 70$ Hz), while above this frequency they accept approximately identical values. This happens due to the monoaural phase effect (worked out by GOLDSTEIN [4]). A significant decrease of threshold values, accompanying an increase of the modulating frequency above 70 Hz is observed, because the spectrum of the modulated signal exceeds the width of one critical band. In such a case the amplitude and frequency modulation are percepted as identical phenomena and the phase effect disappears. As it has been mentioned previously also thresholds of perception of amplitude and frequency modulation obtained with irregular modulating signals have been determined separately. Research results are shown in Figs. 2a and 2b.

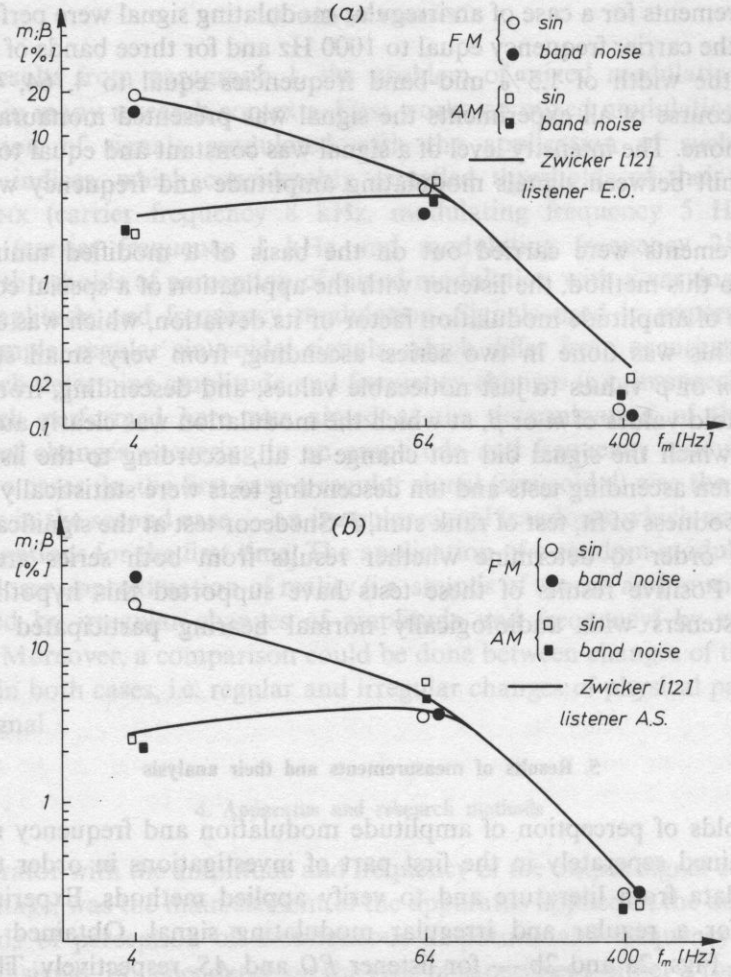

Fig. 2. Thresholds of perception of amplitude (*AM*) and frequency (*FM* modulation for a regular (sinusoidal) and irregular (random) modulating signal in terms of modulating frequency, a — for listener *EO*, b — for listener *AS*

Research was concerned mainly with the determination of thresholds of perception of mixed modulation. To this end, at an adequately chosen subthreshold value of the amplitude modulation factor, the listener himself increased the signal deviation to the moment when he percepted (observed) just noticeable changes of the signal (ascending series), or decreased its value to the moment when he percepted a pure sound (descending series). Subthreshold values of the amplitude modulation factor were equal to

$$0.2\,m_t;\ 0.4\,m_t;\ 0.6\,m_t;\ 0.8\,m_t;\ 1\,m_t$$

(i.e. expressed as a fraction of the threshold value m_t, which has been determined in the first part of research). Figs, 3, 4 and 5 present changes of thresholds of perception

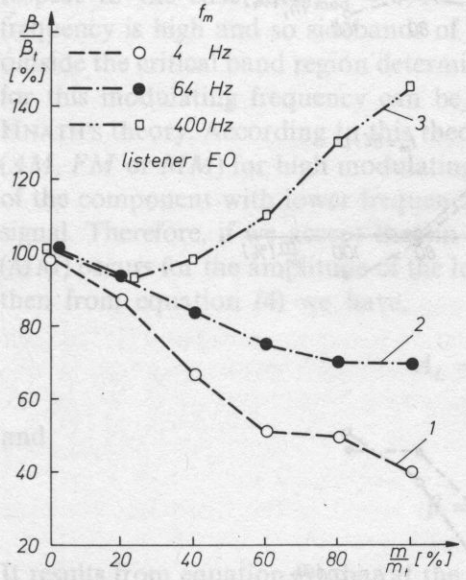

Fig. 3. Thresholds of perception of amplitude–frequency modulation of a tonal signal for listener *EO*, for a regular modulating signal with the following frequencies: 4, 64, 400 Hz

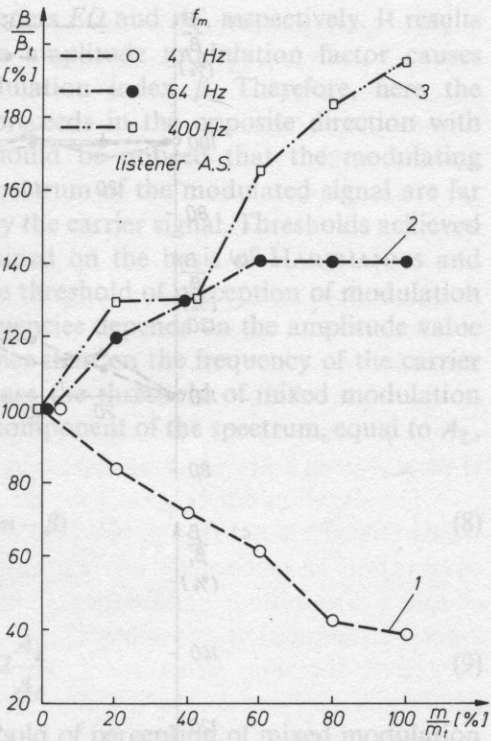

Fig. 4. Thresholds of perception of amplitude-frequency modulation of a tonal signal for listener *AS* for a regular modulating signal with the following frequencies: 4, 64, 400 Hz

of mixed modulation (amplitude-frequency) for regular (Figs. 3, 4) and irregular (Figs. 5) amplitude and frequency changes of the modulated signal. The following quantities are marked on the respective coordinate axes of these diagrams: adequats frequency β and amplitude m modulation indices, normalized with respect to threshold values (β_t, m_t), which were determined in the first part of investigations. Curves marked 1 in Figs. 3 and 4 represent changes of thresholds for a regular modulating signal with frequency $f_m = 4$ Hz, for listeners *EO* and *AS*, respectively. It results from these diagrams that an increase of the amplitude modulation factor m from 0 to the threshold value (i.e. when $m/m_t = 100\%$) for $f_m = 4$ Hz, causes a significant decrease of the frequency modulation index.

Hence, we can infer that in the range of low modulating frequencies, i.e. in the region in which the ear can "follow" the changes of values of signal parameters in time, a coupling is observed in the sense of summation (aid) of sensations produces by both types of modulation under consideration. Or in other words — subthreshold changes of amplitude and subthreshold changes of frequency, which are produced simultaneously in a sinusoidal signal (in the conditions of mixed modulation *MM*),

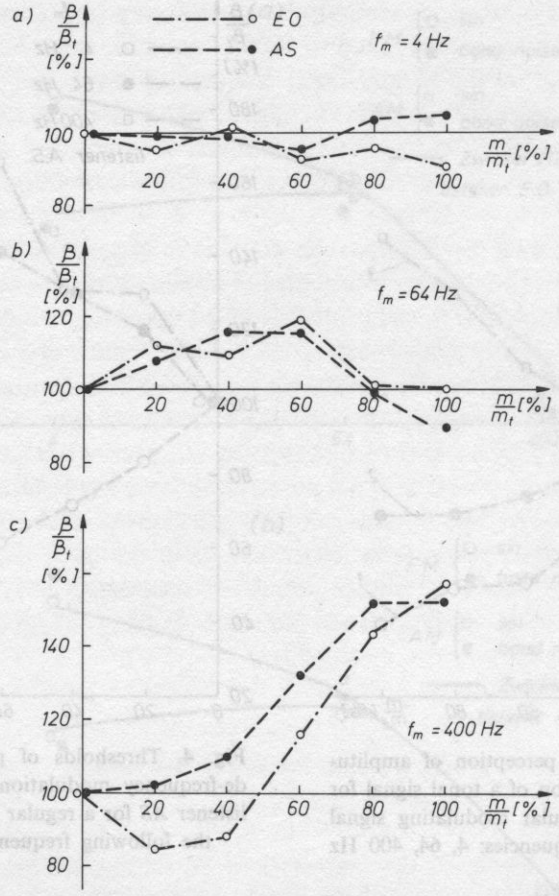

Fig. 5. Thresholds of perception of amplitude-frequency modulation of a tonal signal for listeners *EO* and *AS* for a random modulating signal with mid-band frequency equal to: a — 4 Hz, b — 64 Hz, c — 400 Hz, and width 1.5%

are percepted by listeners for definite values of m and β. Similar relations have been observed by CONINX [1] for threshold values, and ZWICKER [10] for above threshold values.

Such an effect of summation of sensations, created by simultaneous *AM* and *FM* modulation, has not been observed in the case of an irregular modulating signal, i.e. for irregular amplitude and frequency changes of the tone (see Fig. 5a). In this case the *MM* threshold does not depend on occuring changes of the amplitude of the signal, which are determined by the value of the amplitude modulation factor. The divergence of *MM* thresholds for a regular (sinusoidal) and irregular (random) modulating signal is rather surprising, because threshold values determined from separate investigations of amplitude and frequency modulation, were very similar for both types of the modulation signal, i.e. regular and irregular (see Figs. 2a and 2b). Curves marked 3 in Figs. 3 and 4 represent thresholds of mixed modulation for

modulating frequency $f_{mod} = 400$ Hz, for listeners *EO* and *AS*, respectively. It results from these figures that an increase of the amplitude modulation factor causes a distinct increase of the frequency modulation index β. Therefore, here the cooperation of both types of modulation preceeds in the opposite direction with respect to the case for $f_{\mathrm{mod}} = 4$ Hz. It should be noticed that the modulating frequency is high and so sidebands of the spectrum of the modulated signal are far outside the critical band region determined by the carrier signal. Thresholds achieved for this modulating frequency can be explained on the basis of HARTMANN'S and HNATH'S theory. According to this theory the threshold of perception of modulation (*AM*, *FM* or *MM*) for high modulating frequencies depends on the amplitude value of the component with lower frequency, rather than on the frequency of the carrier signal. Therefore, if we accept that in our case the threshold of mixed modulation (*MM*) occurs for the amplitude of the lower component of the spectrum, equal to A_L, then from equation (4) we have,

$$A_L = \frac{A_0}{2}(m-\beta) \tag{8}$$

and

$$\beta = m - 2\frac{A_L}{A_0}. \tag{9}$$

It results from equation (9) that at the threshold of perception of mixed modulation the frequency modulation index is in linear dependence with the amplitude modulation factor m. Such a relationship is presented approximately by curves marked 3 in Figs. 3 and 4.

A similar situation takes place for an irregular modulating signal. Results of investigations for this case are shown in Fig. 5b. Also here the frequency modulation index increases linearly with an increase of the amplitude modulation factor in a certain interval. This proves that the irregular character of rapidly changing physical parameters of the signal does not influence perception significantly. Curves marked 2 in Figs. 3 and 4 represent thresholds of perception of mixed modulation for listeners *EO* and *AS*, respectively, when a sinusoidal signal with frequency $f_{\mathrm{mod}} = 64$ Hz is the modulating signal. It results from these figures that results obtained for both listeners differ in quality. For listener *AS* (Fig. 4) an approximately linear increase of the frequency modulating index β accompanies the increase of the amplitude modulation factor m, while for listener *EO* (Fig. 3) the β value decreases with an increase of m. Therefore, a cooperation of both types of modulation in the sense of their mutual aid, very much like for the modulation frequency of 4 Hz, was stated for listener *EO*, while in the case of listener *AS*, the cooperation has a reverse direction, like for modulating frequency $f_{\mathrm{mod}} = 400$ Hz.

Fig. 5c presents thresholds analogic to those in Figs, 3, 4 (curves marked 2), but in this case a narrow noise band with mid-band frequency equal to 64 Hz is the modulating signal. We can see that an initial increase of the amplitude modulation

factor causes a small rise of the frequency modulation index, what suggests a case analogic to that for $f_{mod} = 400$ Hz, i.e. mutual weakening of sensations created by both types of modulation. However, a further increase of the amplitude modulation factor causes a decrease of β to its initial value, i.e. like for $f_{mod} = 4$ Hz. Presented above results of experiments point to a rather complex mechanism of perception of *MM* modulated signals. The spectral structurs, or in other words — the component with frequency lower than the carrier frequency of the signal, is the factor, which determines the perceptivity of changes in a case of regular amplitude and frequency changes of the signal occuring very quickly (high value of f_{mod}). This means that the component with higher frequency does not influence the perception process at the threshold of perception, although its amplitude is by $A_0\beta$ higher than the amplitude of the lower component. Thus, the component with higher frequency undergoes complete masking by the carrier signal at high modulating frequencies, what HARTMANN and HNATH postulated in their theory [5].

The situation differs greatly for the modulating frequency equal to 4 Hz. In such a case changes of physical parameters occur slowly enough for the ear to "follow" the observation of successiove minima and maxima of loudness and pitch. A positive coupling of amplitude and frequency changes occurs — sensations produced by both types of modulation are summed.

Here, the time structure of the modulated signal is the main factor which determines the perception of *MM* modulation.

The presented above two methods (mechanisms) of perception of modulated signals, have been isolated considering only the value of the modulating frequency. As it has been mentioned above, the time mechanism functions when changes of physical parameters of a signal are relatively slow; while the spectral mechanism functions when these changes are relatively fast. It is possible that these are two independent mechanisms, which can occur seperately, or simultaneously as a certain combination, especially for modulating frequencies from the range of so-called roughness. The transition of the time mechanism into the spectral mechanism is undoubtedly a continuous process, individual for different listeners and dependent on values of modulation frequencies. Data presented in Figs. 3 and 4 (curves marked 2) confirm this. It results from them that for modulating frequency $f_{mod} = 64$ Hz, the spectral mechanism prevails for listener *AS*, while for listener *EO* the time mechanism dominates.

Relationships between adequate modulation indices, which were observed for mentioned values of modulating frequencies, prove that the perception of one type of modulation is not independent from the coexisting second type of modulation.

Research performed does not give a final answer to the question, in which frequency ranges these mechanisms (spectral and time) occur. It is initial research, which tries to explain the method of perception of signals varying in time. A rather arbitrary choice of modulating signals, which was done on the basis of perception ranges of modulated signals widely mentioned in literature, limits investigations to only a part of phenomena accompanying the perception of these kinds of signals.

Therefore, research seems worth continuing, especially in the domain of signals modulated by irregular signals, which as we know constitute a great part of sounds met in practice.

References

[1] E. Coninx, *The detection of combined differences in frequency and intensity*, Acustica, **39**, 3, 138–150 (1977).

[2] F. Coninx, *The perception of combined frequency and amplitude modulation with clearly audible modulation depths*, Acustica, **39**, 3, 151–154 (1977).

[3] A. Czajkowska, *Generalized difference thresholds and valuation of simultaneous changes of intensity and frequency of a tone*, Arch. Akustyki, **16**, 3, 257–266 (1981) (in Polish).

[4] L. J. Goldstein, *Auditory spectral filtering and monaural phase perception*, JASA, **41**, 2, 458–479 (1967).

[5] W. M. Hartmann, G. H. Hnath, *Detection of mixed modulation*, Acustica, **50**, 5, 297–312 (1982).

[6] D. Maiwald, *Ein Funktionsschema des Gehörs zur Beschreibung der Erkennbarkeit kleiner Frequenz und Amplitudenanderungen*, Acustica, **18**, 2, 81–92 (1967).

[7] D. Maiwald, *Die Berechnung von Modulationsschwellen mit Hilfe eines Funktionsschemas*, Acustica, **18**, 4, 193–207 (1967).

[8] A. R. Moller, *Coding of amplitude and frequency modulated sounds in the cochlear nucleus*, Acustica, **31**, 6, 292–299 (1974).

[9] A. R. Moller, *Frequency selectivity of single auditory–nerve fibres in response to broadband noise stimuli*, JASA, **62**, 1, 135–142 (1977).

[10] E. Ozimek, A. Sęk, *Perception of irregular changes of sinusoidal signals* (paper sent to Acustica).

[11] E. Zwicker, *Direct comparison between the sensation produced by frequency modulation and amplitude modulation*, JASA, **34**, 8, 1425–1430 (1962).

[12] E. Zwicker, *Die Grenzen der Hörbarkeit der Amplitudemodulation und der Frequenzmodulation eines Tones*, Acustica, **2**, 3, 125–133 (1952).

Received on March 26, 1986; revised version on October 14, 1986

ARCHIVES OF ACOUSTICS
12, 1, 17–31 (1987)

PROPAGATION VELOCITY OF A VIBRATION VELOCITY WAVE, I.E. ACOUSTIC VELOCITY WAVE

ROMAN WYRZYKOWSKI

Institute of Physics, Pedagogic High School in Rzeszów
(35–310 Rzeszów, ul. Rejtana 16a)

In this paper the author proves that the propagation velocity of an acoustic velocity wave in the near field differs from the velocity of a pressure wave, while both differ from c_0 in d'Alambert's equation. The velocity of an acoustic velocity wave was calculated for a point source, for a cylindrical source of zero order and for a circular piston and ring in a baffle.

1. Introduction

In accordance with papers [8, 9], an arbitrary tensor physical quantity $p_{ijk...}$ which propagates in the form of a harmonic wave, can be noted as follows

$$p_{ijk...} = A_{ijk...}(x_i)e^{i[\omega t - f(x_i)]} \tag{1}$$

where $A_{ijk...}(x_i)$ is the amplitude in terms of position, and $f(x_i)$ represents the so-called wave front. The wave propagation condition is [4, 5, 7]:

$$\omega t - f(x_i) = \text{const} \tag{2}$$

what leads to an expression for the local velocity (velocity dependent on the position of the point in the acoustic field)

$$c = \omega/|\text{grad} f|. \tag{3}$$

If we write (1) for an acoustic pressure wave:

$$p = P_0(x_i)e^{i[\omega t - f(x_i)]} \tag{4}$$

which propagates with a velocity given in formula (3), then we can easily prove that in a general case a vibration velocity wave propagates with a different velocity. As we know [3–6], the vibration velocity, called also the acoustic velocity, is related to the acoustic pressure by Euler's equation, which has the following form the a harmonic

wave

$$u = \frac{i}{\omega \varrho_0} \operatorname{grad} p \tag{5}$$

where ϱ_0 is the rest desity of the medium.

Both, the amplitude and the phase, are differentiated when the gradient of expression (4) is calculated. If we convert the obtained result into a form analogic to formula (1) we have:

$$u = U_0(x_i) e^{i[\omega t - f_1(x_i)]}. \tag{6}$$

Hence, when a pressure wave propagates with velocity (3) (where $f(x_i)$ will be the value of the wave front function from formula (4)), the velocity wave propagates with velocity

$$c_u = \omega / |\operatorname{grad} f_1| \tag{7}$$

where $f_1(x_i)$ is a different function — the function of the wave front of an acoustic velocity wave from formula (6).

It will be shown below that c_u differs from c for all waves (except plane waves) only at relatively small distances, when the local velocity of a pressure wave c differs from the material velocity c_0.

M. KWIEK [3] calculated the propagation velocity of a velocity wave for a point source, considering this as a special case and neglecting the generality of the problem. His calculation procedure is given in paragraph 2.

2. Propagation velocity of a velocity wave in the field of a point source

This example has been chosen purposely, because as we know the acoustic pressure wave of a point source is an elementary spherical wave, which propagates with a constant velocity, in paper [7] called the material velocity. The behaviour of the propagation velocity of a velocity wave in such a case is very interesting. The acoustic pressure at a distance r from the point source [6] equals

$$p = (A/r) e^{i(\omega t - k_0 r)} \qquad k_0 = \omega / c_0 \tag{8}$$

of course a point source is an abstract source, but it can be replaced in practice by a very small pulsating sphere.

Applying Euler's equation (5) in (8) we obtain the acoustic velocity

$$u = \frac{1}{\varrho c_0} \left(1 + \frac{1}{i k_0 r}\right) \frac{A}{r} e^{i(\omega t - k_0 r)}. \tag{9}$$

By separating the absolute value and the phase we bring formula (9) to a form analogic to (1)

$$u = \frac{A}{\varrho c_0 r} \sqrt{1 + \frac{1}{(k_0 r)^2}}\, e^{i\left(\omega t - k_0 r - \operatorname{tg}^{-1} \frac{1}{k_0 r}\right)} \tag{10}$$

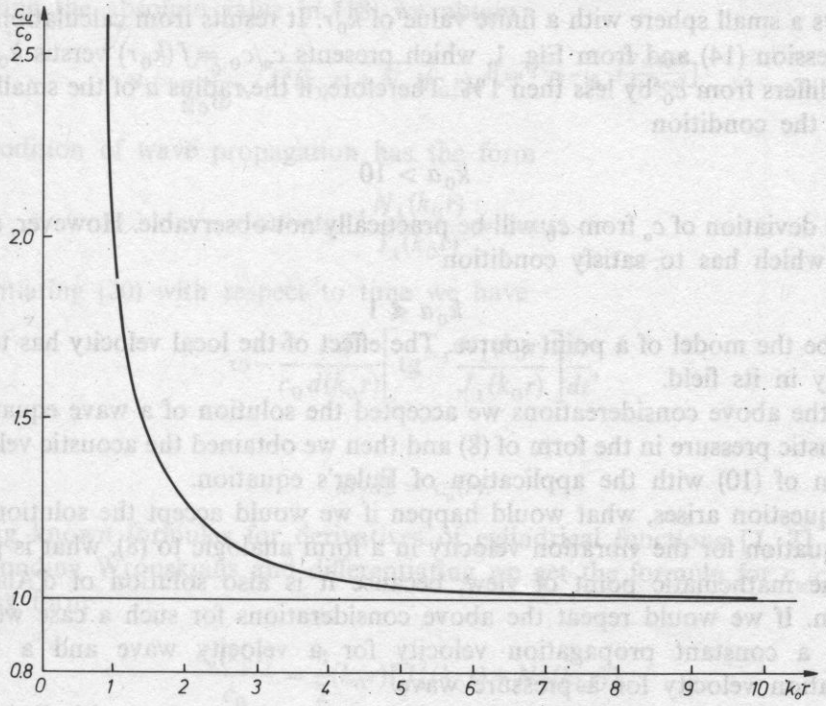

Fig. 1. c_u/c_0 versus k_0r for a point source

where tg^{-1} denotes arctg. The condition of wave propagation requires r and t to change in such a manner so the total phase remains constant, thus

$$\omega t - k_0 r - \mathrm{tg}^{-1}\frac{1}{k_0 r} = \text{const.} \tag{11}$$

Differentiating both sides of (11) with respect to time we have

$$\omega - k_0 \cdot \frac{dr}{dt} + \frac{k_0}{1+\left(\frac{1}{k_0 r}\right)^2} \cdot \frac{1}{(k_0 r)^2} \cdot \frac{dr}{dt} = 0. \tag{12}$$

Since

$$dr/dt = c_u \tag{13}$$

thus finally

$$c_u(k_0 r)/c_0 = [1+(k_0 r)^2]/(k_0 r)^2, \tag{14}$$

when $k_0 r \to 0$, $c_u/c_0 \to \infty$. This is not surprising, because the acoustic pressure p (8) and the vibration velocity (10) exhibits singularity at $r = 0$. Therefore, it is also not surprising that the propagation velocity c_u exhibits singularity in this point as well. Whereas, when $k_0 r \to \infty$ we have according to expactations $c_u \to c_0$. In practice there

is always a small sphere with a finite value of $k_0 r$. It results from calculations based on expression (14) and from Fig. 1, which presents $c_u/c_0 = f(k_0 r)$ versus $k_0 r > 10$, that c_u differs from c_0 by less then 1%. Therefore, if the radius a of the small sphere satisfies the condition

$$k_0 a > 10 \tag{15}$$

then the deviation of c_u from c_0 will be practically not observable. However, a small sphere, which has to satisfy condition

$$k_0 a \ll 1 \tag{16}$$

should be the model of a point source. The effect of the local velocity has to occur distinctly in its field.

In the above considereations we accepted the solution of a wave equation for the acoustic pressure in the form of (8) and then we obtained the acoustic velocity in the form of (10) with the application of Euler's equation.

A question arises, what would happen if we would accept the solution of the wave equation for the vibration velocity in a form analogic to (8), what is possible from the mathematic point of view, because it is also solution of d'Alambert's equation. If we would repeat the above considerations for such a case we would achieve a constant propagation velocity for a velocity wave and a variable propagation velocity for a pressure wave.

It should be mentioned that this problem can not be solved with d'Alambert's and Euler's equations solely. Formula (8) for pressure was also obtained with the application of a different method, by differentiating Green's function, which has a definite physical interpretation.

3. Propagation velocity of an acoustic velocity wave in the field of a cylinder for a zero order wave

The acoustic pressure for a cylindrical wave of zero order is expressed by formula [4–6]

$$p = P_0[J_0(k_0 r) - iN_0(k_0 r)]e^{i\omega t}, \tag{17}$$

where P_0 denotes the pressure amplitude, which can be determined from the boundary condition on the surface of the cylinder (source); $J_0(\,)$ and $N_0(\,)$ are zero order Bessel and Neuman functions, respectively; $k_0 = \omega/c_0$. According to Euler's equation (5) the acoustic velocity equals [6, 2]

$$u = \frac{P_0}{\varrho_0 \omega} e^{i(\omega t + \frac{3}{2}\pi)}[J_1(k_0 r) - iN_1(k_0 r)], \tag{18}$$

where $J_1(\,)$ and $N_1(\,)$ are first order Bessel and Neuman functions, respectively.

Separating the absolute value in (18) we obtain

$$u = \frac{P_0}{\varrho_0 \omega} \sqrt{J_1^2(k_0 r) + N_1(k_0 r)}\, e^{i\left[\omega t + \frac{3}{2}\pi - \mathrm{tg}^{-1}\frac{N_1(k_0 r)}{J_1(k_0 r)}\right]}. \tag{19}$$

The condition of wave propagation has the form

$$\omega t - \mathrm{tg}^{-1}\frac{N_1(k_0 r)}{J_1(k_0 r)} = \text{const.} \tag{20}$$

Differentiating (20) with respect to time we have

$$\omega - \frac{\omega}{c_0}\frac{d}{d(k_0 r)}\left[\mathrm{tg}^{-1}\frac{N_1(k_0 r)}{J_1(k_0 r)}\right]\frac{dr}{dt}, \tag{21}$$

where

$$dr/dt = c_u(r). \tag{22}$$

Applying known formulas for derivatives of cylindrical functions [1, 2] and for corresponding Wronskians and differentiating we get the formula for c_u/c_0 in the following form

$$\frac{c_u(k_0 r)}{c_0} = \frac{\pi}{2}(k_0 r)[J_1^2(k_0 r) + N_1^2(k_0 r)]. \tag{23}$$

When $k_0 r \to \infty$, in accordance with asymptotic formulae for cylindrical functions [1, 2] we have

$$J_1^2(k_0 r) + N_1^2(k_0 r) = 2/(\pi k_0 r) \qquad k_0 \gg 1 \tag{24}$$

and then we get from (23)

$$c_u/c_0 = 1 \qquad k_0 r \gg 1. \tag{25}$$

Whereas for small $k_0 r \ll 1$ we have

$$J_1(k_0 r) = 0 \qquad k_0 r \ll 1, \tag{26}$$

$$N_1(k_0 r) = \frac{1}{\pi}\frac{2}{k_0 r} \tag{27}$$

and from (23)

$$c_u/c_0 \to \infty \qquad k_0 r \to 0. \tag{28}$$

Of course $k_0 r = 0$ is only a mathematical limit without physical sense and (28) proves inly that the local velocity c_u exhibits singularity for $k_0 r = 0$.

Fig. 2 presents the function $c_u/c_0 = f(k_0 r) c_u$ differs from c_0 by less than 1% for values of $k_0 r$ higher than $k_0 r = 7$. Therefore, if a cylinder which radiates a zero order wave has a radius, a, which satisfies the condition $k_0 a > 7$, then the local velocity effect of a velocity wave practically will not occur. Whereas, for $k_0 a < 7$ this velocity

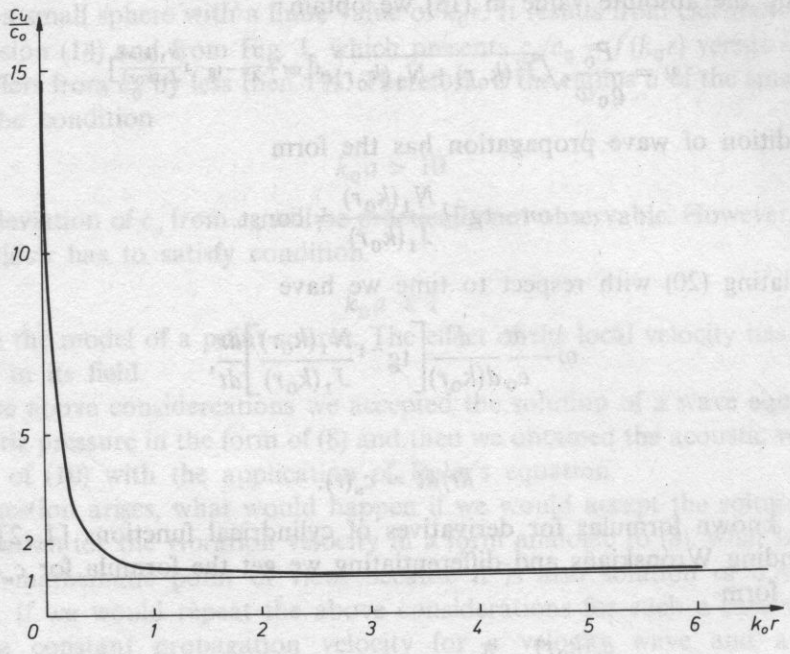

Fig. 2. c_u/c_0 versus $k_0 r$ for a cylindrical wave of zero order

will be reduced with the distance from the source to the value c_0, but this velocity will differ from the propagation velocity of a pressure wave. It has been shown in paper [7] that the velocity of a pressure wave increases from 0 to c_0.

4. Phase velocity of an acoustic velocity wave on the axis of symmetry of the field produced by a circular piston in a rigid baffle

As in papers [7, 8], we will consider a circular piston with radius a vibrating with a constant amplitude of vibration velocity u_0, and situated in an infinite plane rigid baffle. Axis z drawn from the center of the piston perpendicularly to its surface is identical with the axis of symmetry of the obtained acoustic field. The propagation velocity of a velocity wave (c_u) was calculated with the application of a formula for the acoustic pressure on the axis z for the field, given in a compact form by STENZEL [5, 6].

It to simplify the notation we will accept the formula given by STENZEL [5, 6] for the relative acoustic pressure

$$p_w = \frac{p}{\varrho_0 c_0 u_0} = 2\sin\left[\frac{k_0}{2}\left(\sqrt{a^2+z^2}-z\right)\right] e^{i\left[\omega t+\frac{\pi}{2}-\frac{k_0}{2}\left(\sqrt{a^2+z^2}+z\right)\right]}. \tag{29}$$

where ϱ_0 is the rest density of the medium, u_0 is the amplitude of vibration velocity, which is constant on the source, $k_0 = \omega/c_0$.

In accordance to Euler's equation (5) we have

$$u = \frac{1}{\omega\varrho} e^{i\frac{\pi}{2}} \frac{dp}{dz} = U_0 \frac{dp_w}{dz}. \tag{30}$$

Further calculations are simplified by the fact that we only need the expression for the phase of u in order to determine the formula for the propagation velocity c_u.

After differentiating (29) with respect of z, we see that the total velocity phase can be expressed by

$$\varphi(z, t) = \omega t - \frac{k_0}{2}\left(\sqrt{a^2+z^2}+z\right) + \operatorname{tg}^{-1}\left\{\operatorname{tg}\left[\frac{k_0}{2}\left(\sqrt{a^2+z^2}-z\right)\right]\frac{\sqrt{a^2+z^2}+z}{\sqrt{a^2+z^2}-z}\right\} \tag{31}$$

and the condition for the propagation of a velocity wave has the following form

$$\varphi(z, t) = \text{const}. \tag{32}$$

In order to simplify formulas used in the further part of the paper we will denote

$$\varphi(z, t) = \omega t - F(z), \tag{33}$$

where

$$F(z) = \frac{k_0}{2}\left(\sqrt{a^2+z^2}-z\right) - \operatorname{tg}^{-1}\left\{\operatorname{tg}\left[\frac{k_0}{2}\sqrt{a^2+z^2}-z\right]\frac{\sqrt{a^2+z^2}+z}{\sqrt{a^2+z^2}-z}\right\}. \tag{34}$$

Differentiating both sides of (32) with respet to time and substituting $\varphi(z, t)$ in the form given in (33), we obtain

$$\omega - (dF(z)/dz)(dz/dt) = 0, \tag{35}$$

where

$$dz/dt = c_u. \tag{36}$$

Therefore, from (35) we have

$$c_u = \frac{\omega}{dF(z)/dz}. \tag{37}$$

The following notation simplifications were introduced

$$dF/dz = (k_0/2)F_1(z), \tag{38}$$

hence

$$c_u(z)/c_0 = 2/F_1(z), \tag{39}$$

where $F_1(z)$ equals

$$F_1(z) = \frac{\frac{z}{a} + \sqrt{1+\left(\frac{z}{a}\right)^2}}{\sqrt{1+\left(\frac{z}{a}\right)^2}} - \frac{\left[\sqrt{1+\left(\frac{z}{a}\right)^2} - \frac{z}{a}\right]^2}{\left[\sqrt{1+\left(\frac{z}{a}\right)^2} - \frac{z}{a}\right]^2 + \mathrm{tg}^2\left[\frac{k_0 a}{2}\left(\sqrt{1+\left(\frac{z}{a}\right)^2} - \frac{z}{a}\right)\right]\left(\sqrt{1+\left(\frac{z}{a}\right)^2} + \frac{z}{a}\right)^2} \times$$

$$\times \left\{ \frac{2\,\mathrm{tg}\left[\frac{k_0 a}{2}\left(\sqrt{1+\left(\frac{z}{a}\right)^2} - \frac{z}{a}\right)\right]}{\frac{k_0 a}{2}\left[\sqrt{1+\left(\frac{z}{a}\right)^2} - \frac{z}{a}\right]^2 \sqrt{1+\left(\frac{z}{a}\right)^2}} - \right.$$

$$\left. - \left\{1 + \mathrm{tg}^2\left[\frac{k_0 a}{2}\left(\sqrt{1+\left(\frac{z}{a}\right)^2} - \frac{z}{a}\right)\right]\right\} \frac{\sqrt{1+\left(\frac{z}{a}\right)^2} + \frac{z}{a}}{\sqrt{1+\left(\frac{z}{a}\right)^2}} \right\}. \tag{40}$$

For a specific case, when $z/a = 0$, we achieve the following expression

$$F_1(0) = 2\left\{1 - \frac{\mathrm{tg}\left(\frac{k_0 a}{2}\right)}{\frac{k_0 a}{2}\left[1 + \mathrm{tg}^2\left(\frac{k_0 a}{2}\right)\right]}\right\} = 2\left[1 - \frac{\sin(k_0 a)}{k_0 a}\right] \tag{41}$$

and from (27) we have

$$\frac{c_u(0)}{c_u} = \frac{1 + \mathrm{tg}^2\left(\frac{k_0 a}{2}\right)}{1 + \mathrm{tg}^2\left(\frac{k_0 a}{2}\right) - \mathrm{tg}\left(\frac{k_0 a}{2}\right)\Big/\frac{k_0 a}{2}}. \tag{42}$$

At $z = 0$ the value of $c_u(0)$ depends on $k_0 a$. For $k_0 a = 0$ (limiting case without physical sense) we would have $c_u \to \infty$. When $k_0 a \to \infty$, $c_u \to c_0$, in spite of the periodicity of function $\mathrm{tg}(k_0 a/2)$. Fig. 3 presents the dependence $c_u(0)/c_0 = f(k_0 a)$.

As for the full expression (40) we can see that when $z/a \to \infty$, then from formula (27) we obtain at the limit $F_1(\infty) = 2$ and from (27).

$$c_u(\infty)/c_0 = 1. \tag{43}$$

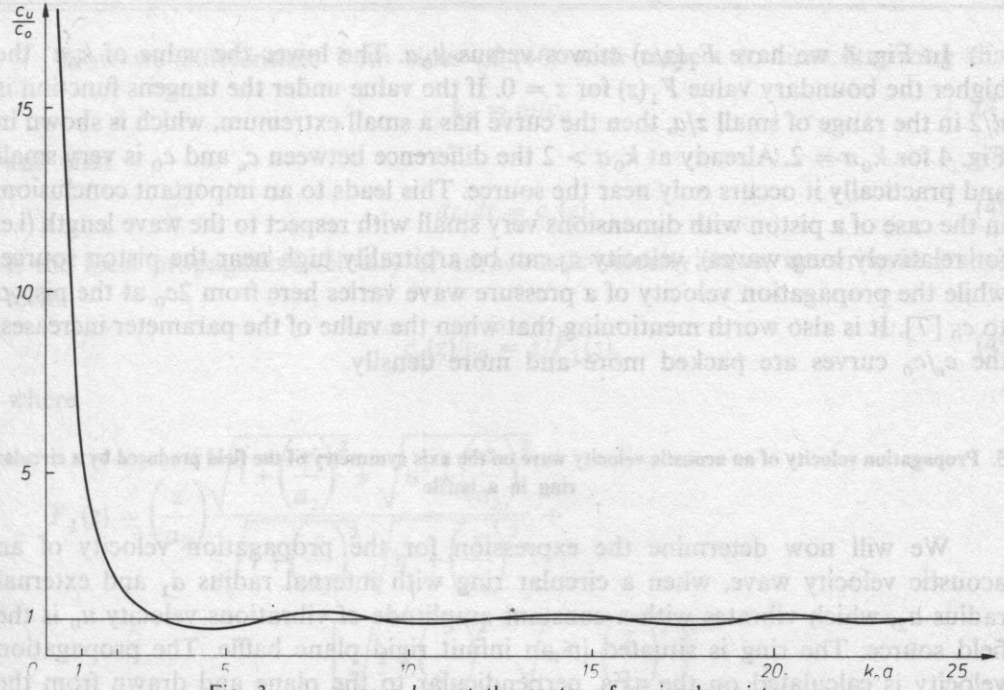

Fig. 3. c_u/c_0 versus k_0a at the center of a circular piston

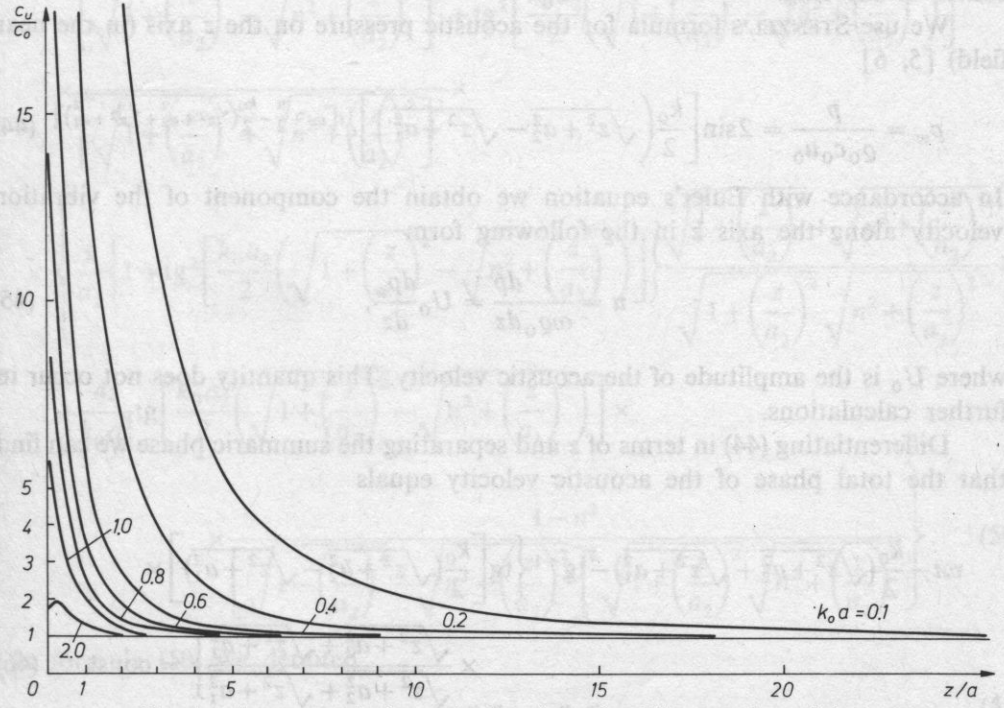

Fig. 4. c_u/c_0 versus z/a for a circular piston for different values of k_0a

In Fig. 4 we have $F_1(z/a)$ curves versus $k_0 a$. The lower the value of $k_0 a$ the higher the boundary value $F_1(z)$ for $z = 0$. If the value under the tangens function is $\pi/2$ in the range of small z/a, then the curve has a small extremum, which is shown in Fig. 4 for $k_0 a = 2$. Already at $k_0 a > 2$ the difference between c_u and c_0 is very small and practically it occurs only near the source. This leads to an important conclusion; in the case of a piston with dimensions very small with respect to the wave length (i.e. for relatively long waves), velocity c_u can be arbitralily high near the piston source, while the propagation velocity of a pressure wave varies here from $2c_0$ at the piston to c_0 [7]. It is also worth mentioning that when the value of the parameter increases, the c_u/c_0 curves are packed more and more densily.

5. Propagation velocity of an acoustic velocity wave on the axis symmetry of the field produced by a circular ring in a baffle

We will now determine the expression for the propagation velocity of an acoustic velocity wave, when a circular ring with internal radius a_1 and external radius a_2, which vibrates with a constant amplitude of vibrations velocity u_0 is the field source. The ring is situated in an infinit rigid plane baffle. The propagation velocity is calculated on the axis, perpendicular to the plane and drawn from the center of the ring.

We use STENZEL'S formula for the acoustic pressure on the z axis (in the near field) [5, 6]

$$p_w = \frac{p}{\varrho_0 c_0 u_0} = 2\sin\left[\frac{k_0}{2}\left(\sqrt{z^2+a_2^2}-\sqrt{z^2+a_1^2}\right)\right] e^{i\left[\omega t+\frac{\pi}{2}-\frac{k_0}{2}\left(\sqrt{z^2+a_2^2}+\sqrt{z^2+a_1^2}\right)\right]} \tag{44}$$

In accordance with Euler's equation we obtain the component of the vibration velocity along the axis z in the following form

$$u = \frac{i}{\omega\varrho_0}\frac{dp}{dz} = U_0\frac{dp_w}{dz}, \tag{45}$$

where U_0 is the amplitude of the acoustic velocity. This quantity does not occur in further calculations.

Differentiating (44) in terms of z and separating the summaric phase we can find that the total phase of the acoustic velocity equals

$$\omega t-\frac{k_0}{2}\left(\sqrt{z^2+a_2^2}+\sqrt{z^2+a_1^2}\right)-\operatorname{tg}^{-1}\left\{\operatorname{tg}\left[\frac{k_0}{2}\left(\sqrt{z^2+a_2^2}-\sqrt{z^2+a_1^2}\right)\right]\times\right.$$
$$\left.\times\frac{\sqrt{z^2+a_2^2}+\sqrt{z^2+a_1^2}}{\sqrt{z^2+a_2^2}+\sqrt{z^2+a_1^2}}\right\} = \text{const.} \tag{46}$$

The constancy of the total phase of acoustic velocity is the condition for wave propagation.

Now we differentiate both sides of (46) with respect to time, knowing that

$$k_0 = \omega/c_0 \tag{47}$$

and that

$$dz/dt = c_u(z) \tag{48}$$

is the local propagation velocity of an acoustic velocity wave, we write in a short form:

$$c_u(z)/c_0 = z/F_1(z), \tag{49}$$

where

$$F_1(z) = \left(\frac{z}{a_2}\right)\frac{\sqrt{1+\left(\frac{z}{a_2}\right)^2}+\sqrt{n^2+\left(\frac{z}{a_2}\right)^2}}{\sqrt{1+\left(\frac{z}{a_2}\right)^2}\sqrt{n^2+\left(\frac{z}{a_1}\right)^2}} +$$

$$+\frac{\left[\sqrt{1+\left(\frac{z}{a_2}\right)^2}-\sqrt{n^2+\left(\frac{z}{a_2}\right)^2}\right]^2}{\left[\sqrt{1+\left(\frac{z}{a_2}\right)^2}-\sqrt{n^2+\left(\frac{z}{a_2}\right)^2}\right]^2+\mathrm{tg}^2\left[\frac{k_0 a_2}{2}\left(\sqrt{1+\left(\frac{z}{a_2}\right)^2}-\sqrt{n^2+\left(\frac{z}{a_2}\right)^2}\right)\right]}\times$$

$$\times\frac{}{\left[\sqrt{1+\left(\frac{z}{a_2}\right)^2}+\sqrt{n^2+\left(\frac{z}{a_2}\right)^2}\right]^2}\times$$

$$\times\left\{\frac{z}{a_2}\left\{1+\mathrm{tg}^2\left[\frac{k_0 a_2}{2}\left(\sqrt{1+\left(\frac{z}{a_2}\right)^2}-\sqrt{n^2+\left(\frac{z}{a_2}\right)^2}\right)\right]\right\}\frac{\sqrt{1+\left(\frac{z}{a_2}\right)^2}+\sqrt{n^2+\left(\frac{z}{a_2}\right)^2}}{\sqrt{1+\left(\frac{z}{a_2}\right)^2}\sqrt{n^2+\left(\frac{z}{a_2}\right)^2}}+\right.$$

$$+\frac{4z}{k_0 a_2^2}\mathrm{tg}\left[\frac{k_0 a_2}{2}\left(\sqrt{1+\left(\frac{z}{a_2}\right)^2}-\sqrt{n^2+\left(\frac{z}{a_1}\right)^2}\right)\right]\times$$

$$\left.\times\frac{1-n^2}{\left[\sqrt{1-\left(\frac{z}{a_2}\right)^2}-\sqrt{n^2+\left(\frac{z}{a_2}\right)^2}\right]^2\sqrt{1+\left(\frac{z}{a_2}\right)^2}\sqrt{n^2+\left(\frac{z}{a_2}\right)^2}}\right\}. \tag{50}$$

In formula (50) we denoted

$$a_1 = n\,a_2 \quad n < 1. \tag{51}$$

For $n = 0$ the ring changes into a circular piston and formula (50) is transformed into formula (40).

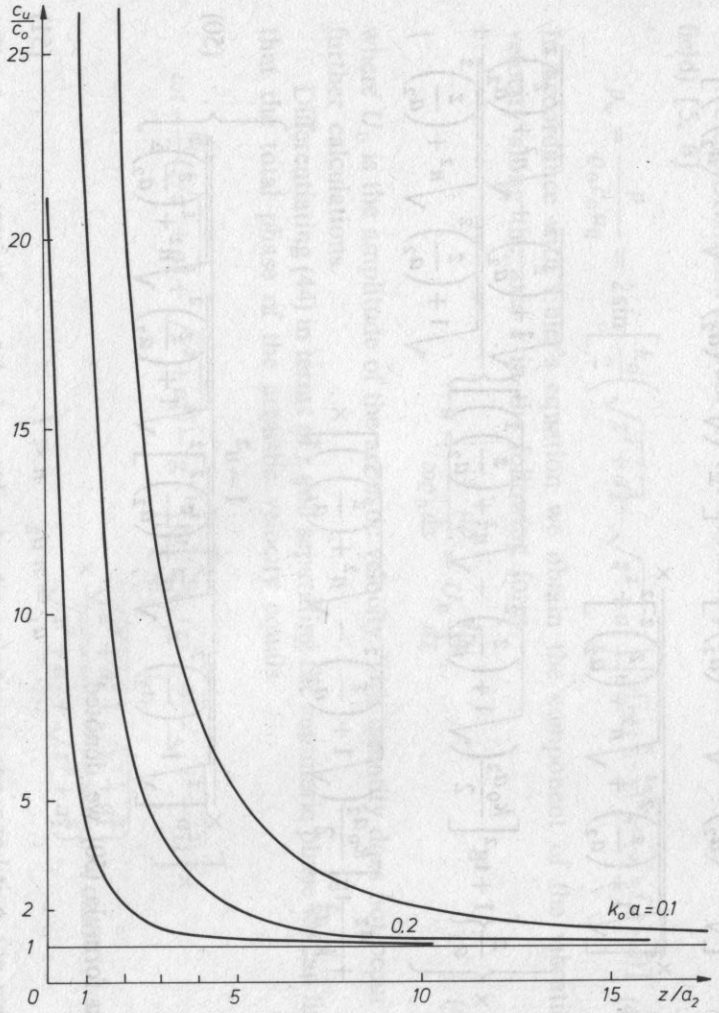

Fig. 5. c_u/c_0 versus z/a_2 for a circular ring, for $k_0 a = 0.1$ and 0.2

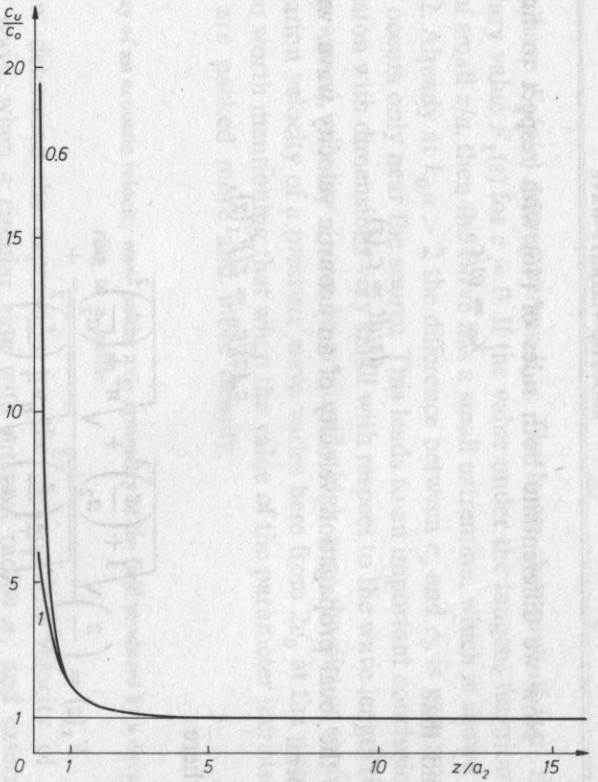

Fig. 6. c_u/c_0 versus z/a_2 for a circular ring for $k_0 a = 1$

[29]

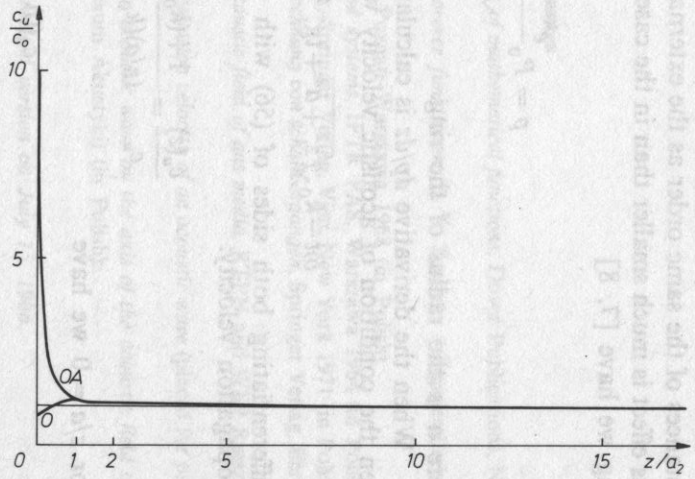

Fig. 7. c_u/c_0 versus z/a_2 for a circular ring for $k_0 a = 5$

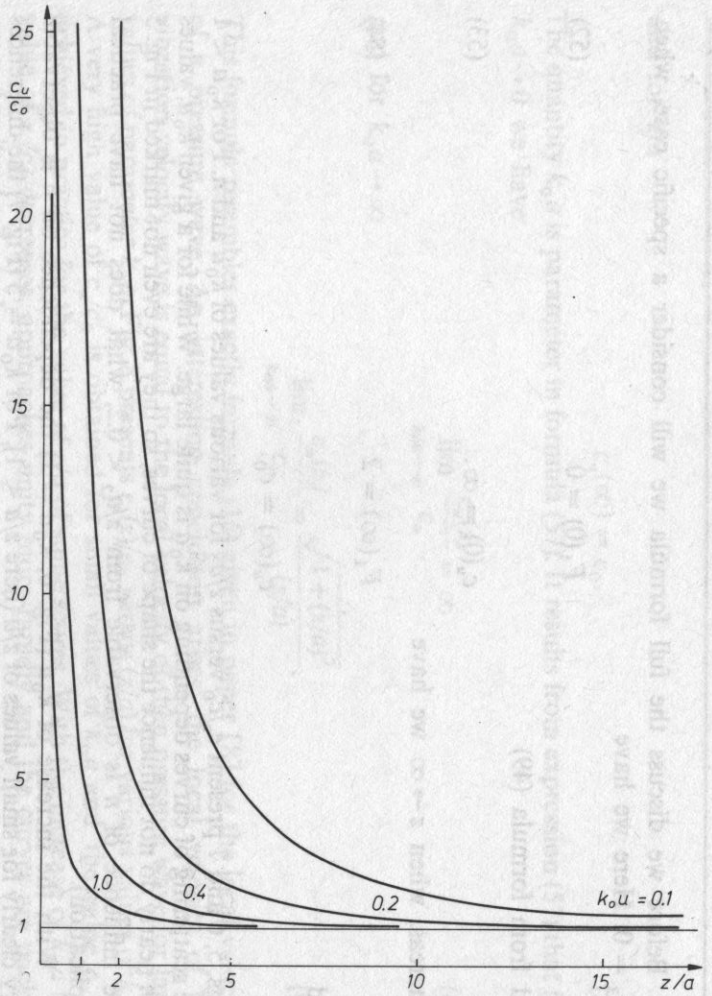

Fig. 8. c_u/c_0 versus z/a for a ring densly packed with point sources

Before we discuss the full formula we will consider a specific case, when $z/a_2 = 0$. Here we have

$$F_1(0) = 0 \tag{52}$$

and from formula (49)

$$c_u(0) = \infty. \tag{53}$$

Whereas, when $z \to \infty$ we have

$$F_1(\infty) = 2 \tag{54}$$

and

$$c_u(\infty) = c_0.$$

Figs. 5, 6 and 7 present c_u/c_0 versus z/a_2 for various values of $k_0 a$ and n. For $k_0 a < 1$ the scattering of curves depending on $k_0 a$ is quite large. While for a given $k_0 a$, values of n nearly do not influence the shape of curves, so they are even not marked in Fig. 5 (the influence of n is observable from $z/a_2 < 0.2$, what does not have practical application).

With the increase of $k_0 a$ (Fig. 6, $k_0 a = 1$) the dependence on n is observable very clearly for small values of z/a (here $z/a < 1$). For $k_0 a = 5$ (Fig. 7) the differences between the oridinates of curves for $n = 0$ and $n = 0.4$ are even greater, but also only up to $z/a = 1$. Hence, the effect of the local velocity of a wave occurs here only at distances of the same order as the external radius of the ring, from the surface. But this effect is much smaller than in the case of a pressure wave. For an infinitely thin ring we have [7, 8]

$$p = P_0 \frac{e^{i(\omega t - k_0 \sqrt{z^2 + a^2})}}{\sqrt{z^2 + a^2}}, \tag{55}$$

were a is the radius of the ring.

When the derivative dp/dz is calculated and the full phase angle is separated, then the condition of acoustic velocity wave propagation has the following form

$$\omega t - k_0 \sqrt{z^2 + a^2} + \operatorname{tg}^{-1}\left(k_0 \sqrt{z^2 + a^2}\right) = \text{const}. \tag{56}$$

Differentiating both sides of (56) with respect to time we achieve the relative propagation velocity:

$$\frac{c_u(z)}{c_u} = \frac{1 + (k_0 a)^2 [1 + (z/a)^2}{(z/a)(k_0 a)^2 \sqrt{1 + (z/a)^2}}. \tag{57}$$

For $z/a = 0$ we have

$$c_u(0) = \infty \tag{58}$$

and for z/a

$$c_u(\infty) = c_0. \tag{59}$$

The quantity $k_0 a$ is parameter in formula (57). It results from expression (57) that for $k_0 a \to 0$ we have

$$\lim_{k_0 a \to \infty} \frac{c_u(z)}{c_u} = \infty \tag{60}$$

and for $k_0 a \to \infty$

$$\lim_{k_0 a \to \infty} \frac{c_u(z)}{c_0} = \frac{\sqrt{1+(z/a)^2}}{(z/a)}. \tag{61}$$

This formula resembles exactly formula (16) given in paper [8] for the local velocity of a pressure wave. An interesting conclusion arises: the local velocity of the vibration velocity wave is equal to the local velocity of then pressure wave for large values of parameter $k_0 a$. Fig. 8 presents $c_u(z)/c_0$ versus (z/a) for various values of $k_0 a$. A very high value of c_u/c_0 is obtained for small values of $k_0 a$ and the value c_0 is achieved in practice for the value of z/a of some scores. With the increase of $k_0 a$ the value of c_u/c_0 decreases, approaches unity more rapidly and the curves are packed more densily. As it can be seen in the figure, it is not purposeful to draw curves for $k_0 a > 1$, because it would only complicate the picture and large differences between c_u and c_0 would only for $z/a \ll 1$.

References

[1] M. ABRAMOWITZ, I. A. STEGUN, *Handbook of mathematical functions*, Dover Publications, New York 1963.

[2] F. JANKE, F. EMDE, F. LOACH, *Tafeln horerer funktionen*, B. 6. Teubner velagagesellschaft, Stuttgard 1960.

[3] M. KWIEK, *Laboratory acoustics*, PWN, Poznań–Warszawa 1968 (in Polish).

[4] I. MALECKI, *Theory, of acoustic waves and systems*, IFTR PAS, Warszawa 1964 (in Polish).

[5] E. SKUDRZYK, *The foundations of acoustics*, Springer Verlag, Vien, New York 1971 (in Polish).

[6] M. STENZEL, O. BROSZE, *Leitfaden zur berechnung von schallvorgangen*, Springer Verlag, Berlin, Heidelberg 1958.

[7] R. WYRZYKOWSKI, *Linear theory of the acoustic field of gas media*, RTPN and WSP Rzeszów 1972 (in Polish).

[8] R. WYRZYKOWSKI, *Position-dependent propagation velocity of an acoustic wave* (placed for print in Archiwum Akustyki) (in Polish).

[9] R. WYRZYKOWSKI, *The local velocity of an acoustic wave on the axis of the acoustic field of a sircular ring in a baffle* (placed for print in Archiwum Akustyki) (in Polish).

Received on February 14, 1986; revised version on July 15, 1986.

ARCHIVES OF ACOUSTICS
12, 1, 33–51 (1987)

RECTANGULAR PHASE SOUND SOURCES FOCUSING RADIATED ENERGY OF VIBRATIONS

ANDRZEJ PUCH

Institute of Physics, Higher Pedagogical School in Rzeszów
(35–310 Rzeszów, ul. Rejtana 16a)

This paper is concerned with the acoustic field in the Fresnel zone of a focusing rectangular phase sound source with the following amplitude distributions of the vibration velocity: uniform, HAMMING'S, HANNING'S and BLACKMAN'S. Amplitude distributions of the acoustic potential were determined along the main axis of such a sound source and in planes parallel to the main axis. It was found that in the case of HAMMING'S, HANNING'S and BLACKMAN'S amplitude distributions of the vibration velocity, the amplitude distribution of the acoustic potential along the amin axis has only one maximum, which is situated near the focal point. This maximum has the highest value for HAMMING'S distribution. When the dimensions of the source are increased, the value of the maximum increases and it is shifted towards the focal point, while its width decreases. Amplitude distributions of the acoustic potential in planes parallel to the axis of the source have relatively narrow maxima, which occur along this axis. They are narrower than for a Gaussian amplitude distribution of the vibration velocity, which was analysed in previous papers. Besides the main maximum also side maxima occur in the focal plane. They are strongly damped for HAMMING'S, HANNING'S and BLACKMAN'S distributions.

Therefore, the acoustic field of a focusing rectangular phase sound source with HAMMING'S, HANNING'S and BLACKMAN'S distributions is relatively uniform in the Fresnel zone.

1. Introduction

In order to achieve the highest possible transverse resolving power of ultrasonic diagnostic systems, sources are applied, which essure the radiation of a possibly narrow beam of ultrasonic waves with a homogeneous internal structure, i.e. without local maxima and minima. HASELBERG and KRAUTKRÄMER have proved [3] that a plane sound source with a Gaussian distribution of the amplitude of vibration velocity radiates a wave beam with the required internal structure. Also a spherical, focusing sound source with a Gaussian distribution of the amplitude of vibration velocity can produce a relatively narrow beam of ultrasonic waves with an uniform

internal structure, as it was shown by FILIPCZYŃSKI and ETIENNE [2]. Paper [9] deals with the far acoustic field of a rectangular sound source with the following distributions of the amplitude of vibration velocity: uniform, HAMMING'S, HANNING'S and BLACKMAN'S. It was found that the directional pattern of such a source with HANNING'S distribution has a relatively narrow main maximum and sufficiently damped side maxima. It was also shown that a sound source, which radiates the energy of vibrations to the far field with a sufficiently large directionality can be realized by a rectangular mosaic system of plane sound sources with discrete HANNING'S distributions of their relative bulk efficiencies. This paper investigates the near field of a rectangular phase source with uniform, HAMMING'S, HANNING'S and BLACKMAN'S distributions of the amplitude of vibration velocity. Results obtained prove further research on the possibility of producing a focusing sound source in the form of a rectangular mosaic phase system of planar sound sources worth continuing.

2. The acoustic field of a plane sound source in Fresnel's zone

Let us assume (Fig. 1) that a plane sound source σ_0, which vibrates with a simple periodic motion with frequency f_0, is situated on plane $z = 0$, which is a perfectly rigid baffle S_0. Let it radiate energy of vibrations into half-space $z > 0$, filled with a lossless and homogeneous fluid medium, in which the acoustic wave propagates with velocity c. It was also accepted that the sound source σ_0 in the plane of the baffle S_0 produces an amplitude distribution of the normal component of the vibration velocity described by the following function

$$\begin{aligned} &\varkappa(x, y) \neq 0 \text{ for the surface } \sigma_0; \\ &\varkappa(x, y) = 0 \text{ for the rest of the baffle } S_0. \end{aligned} \tag{1}$$

Let us consider an arbitrary plane S_z in the half-space $z > 0$, parallel to the plane of the baffle S_0 (Fig. 1). z will denote the distance between these two planes. The distribution of the complex amplitude of the acoustic potential in an arbitrary plane S_z can be determined from [4, 10]

$$\Phi(\xi, \eta) = \int_{-\infty}^{+\infty} \int_{-\infty}^{+\infty} \varkappa(x, y) \frac{\exp(j2\pi\nu d)}{2\pi d} dx dy, \tag{2}$$

where $\nu = f_0/c$ is the spatial frequency. It results from Fig. 1 that the distance between point P_z on plane S_z and point P_0 on baffle S_0 is determined from expression

$$d = z\sqrt{1 + \frac{(x-\xi)^2 + (y-\eta)^2}{z^2}}. \tag{3}$$

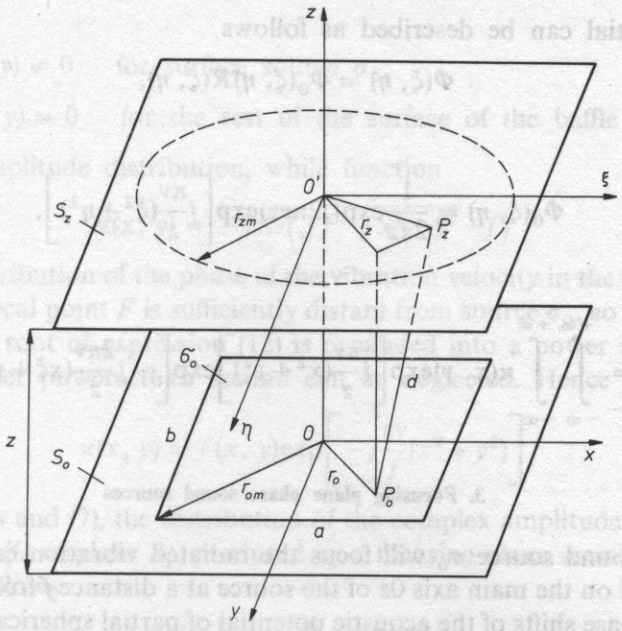

Fig. 1. Plane sound source σ_0 located in baffle S_0 radiating energy of vibrations into a medium which fills the half-space above the baffle

By r_{om} we denote (Fig. 1) the greatest distance of points of the source contour σ_0 from the origin of coordinates, and by r_{zm} — the radius of the neighbourgood of point 0' in which axis $0z$ passes through plane S_z. Let $r_{om} \gg \lambda/v$, where λ is the wave length. It was assumed that the distance z is great enough in relation to r_{om} and r_{zm}, so that all terms with a power greater than two can be neglected in the expansion of the root of expression (3) into a power series. In this case, at $r_o \leqslant r_{om}$ and $r_z \leqslant r_{zm}$ it can be accepted in approximation that [4, 10]

$$d = z + \frac{\xi^2+\eta^2}{2z} + \frac{x^2+y^2}{2z} - \frac{x\xi+y\eta}{z}, \tag{4}$$

while

$$1/d = 1/z, \tag{5}$$

if $\lambda \ll r_{om}$, $r_z \ll z$.

The zone of the acoustic field of a sound source σ_0, in which mentioned above relations are valid, is called the Fresnel zone. Therefore, it results from what was previously said and from (2), that in an area on plane S_z

$$\xi^2+\eta^2 \leqslant r_{zm}^2 \tag{6}$$

which fulfills condition $r_{zm}/z \ll 1$, the distribution of the complex amplitude of the

acoustic potential can be described as follows

$$\Phi(\xi, \eta) = \Phi_0(\xi, \eta)R(\xi, \eta), \tag{7}$$

where

$$\Phi_0(\xi, \eta) = \frac{1}{2\pi z}\exp(j2\pi\nu z)\exp\left[j\frac{\pi\nu}{z}(\xi^2+\eta^2)\right], \tag{8}$$

while

$$R(\xi, \eta) = \int_{-\infty}^{+\infty}\int_{-\infty}^{+\infty} \varkappa(x, y)\exp\left[j\frac{\pi\nu}{z}(x^2+y^2)\right]\exp\left[-j\frac{2\pi\nu}{z}(x\xi+y\eta)\right]dxdy. \tag{9}$$

3. Focusing plane phase sound sources

A plane sound source σ_0 will focus the radiated vibration energy in the focal point F located on the main axis $0z$ of the source at a distance f from its surface (Fig. 2), if mutual phase shifts of the acoustic potential of partial spherical waves produced

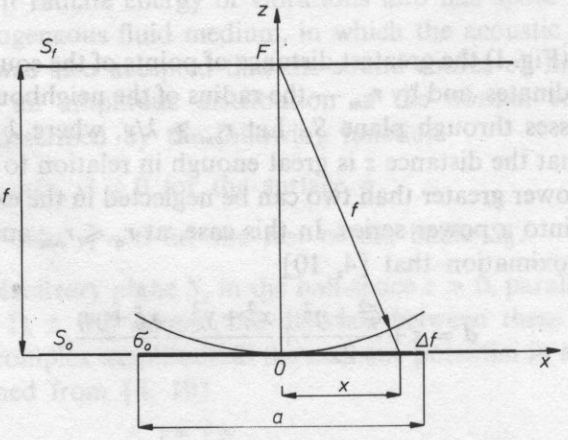

Fig. 2. Determination of the phase distribution of vibration velocity on the surface of a plane focusing phase sound source

by every point of the surface of this source are compensated in point F. This can be obtained by chosing an adequate phase distribution of the vibration velocity on the surface of the source σ_0. It results from Fig. 2 that the plane sound sporce σ_0 will focus the radiated energy of vibrations in focal point F, if the produced by it distribution of the complex amplitude of vibration velocity in the baffle S_0 will be determined as follows

$$\varkappa(x, y) = f(x, y)\exp[j\alpha(x, y)] \tag{10}$$

where function

$$\begin{aligned} f(x, y) &\neq 0 \quad \text{for surface source } \sigma_0; \\ f(x, y) &= 0 \quad \text{for the rest of the surface of the baffle } S_0 \end{aligned} \tag{11}$$

describes the amplitude distribution, while function

$$\alpha(x, y) = -2\pi v\left(\sqrt{f^2+x^2+y^2}-f\right) \tag{12}$$

describes the distribution of the phase of the vibration velocity in the baffle S_0. Let us accept that the focal point F is sufficiently distant from source σ_0, so $r_{om} \ll f$. In such a case when the root of expression (12) is expanded into a power series, all terms which have higher powers than second can be neglected. Hence we have

$$\varkappa(x, y) = f(x, y)\exp\left[-j\frac{\pi v}{f}(x^2+y^2)\right] \tag{13}$$

According to this and (7), the distribution of the complex amplitude of the acoustic potential in area (6) of plane S_z, produced by a focusing plane sound source σ_0 can be written as follows

$$\Phi(\xi, \eta) = \Phi_0(\xi, \eta)R(\xi, \eta), \tag{14}$$

where

$$\Phi_0(\xi, \eta) = \frac{1}{2\pi z}\exp(j2\pi vz)\exp\left[j\frac{\pi v}{z}(\xi^2+\eta^2)\right], \tag{15}$$

while

$$R(\xi, \eta) = \int_{-\infty}^{+\infty}\int_{-\infty}^{+\infty} f(x, y)\exp\left[-j\frac{\pi v}{w}(x^2+y^2)\right]\exp\left[-j\frac{2\pi v}{z}(x\xi+y\eta)\right]dxdy. \tag{16}$$

and

$$1/w = 1/f - 1/z. \tag{17}$$

4. The distribution of the amplitude of the acoustic potential in the focal plane

Let us determine the distribution of the amplitude of the acoustic potential in the region (6) of the focal plane (Fig. 2). In accordance with (9) and (13) we have

$$|\Phi(\xi, \eta)| = |\Phi_0(\xi, \eta)||R(\xi, \eta)|, \tag{18}$$

where

$$\Phi_0(\xi, \eta) = \frac{1}{2\pi f}\exp(j2\pi vf)\exp\left[j\frac{\pi v}{f}(\xi^2+\eta^2)\right] \tag{19}$$

and

$$R(\xi, \eta) = \int_{-\infty}^{+\infty} \int_{-\infty}^{+\infty} f(x, y) \exp\left[-j\frac{2\pi v}{f}(x\xi + y\eta) \right] dxdy. \tag{20}$$

It should be noticed that the right side of the above expression is analogic to a simple two-dimensional Fourier transform. Taking into consideration the spatial spectrum of the amplitude distribution of the vibration velocity in the baffle S_0 we have

$$F(v_x, v_y) = \int_{-\infty}^{+\infty} \int_{-\infty}^{+\infty} f(x, y) \exp[-j2\pi(xv_x + yv_y)] dxdy. \tag{21}$$

Hence, as a result of this and (20) we achieve

$$R(\xi, \eta) = F(v\xi/f, v\eta/f). \tag{22}$$

It results that the amplitude distribution of the acoustic potential in region (6) of the focal plane S_f determines the spatial spectrum of the amplitude distribution of vibration velocity in the baffle S_0. Phase sound source σ_0 under consideration produces (20) in focal point F an acoustic potential with an amplitude equal to

$$|\Phi_F| = F_0/(2\pi f), \tag{23}$$

where

$$F_0 = F(0, 0) = \int_{-\infty}^{+\infty} \int_{-\infty}^{+\infty} f(x, y) dx\, dy \tag{24}$$

is the bulk efficiency of this source which is situated in baffle S_0.

Let us now assume that the focusing phase sound source σ_0 is of rectangular shape with sides: a and b (Fig. 1) and then let us determine the influence of the amplitude distribution of vibration velocity in the baffle S_0, which contains this source, on the amplitude distribution of the acoustic potential in region (6) of the focal plane S_f. The following distributions will be considered: unform, HAMMING'S, HANNING'S and BLACKMAN'S. The influence of these distributions on the far field of a rectangular sound source has been analysed in paper [9]. For comparison let us also take into consideration the Gaussian distribution, which was analysed in papers [2, 3].

a) Uniform distribution. Let us accept that the amplitude distribution of vibration velocity in the baffle is expressed as follows (Fig. 3)

$$f(x, y) = \varkappa_0 f(x) f(y), \tag{25}$$

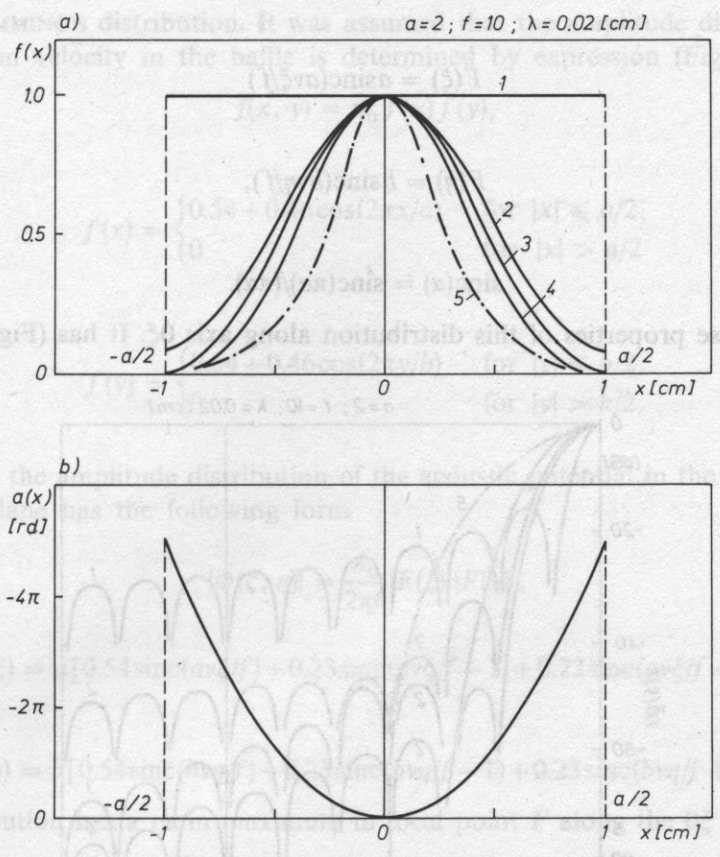

Fig. 3. Amplitude distributions a) and phase distributions b) of the vibration velocity on the surface of a focusing rectangular phase sound source: 1 — uniform, 2 — HAMMING'S, 3 — HANNING'S, 4 — BLACKMAN'S, 5 — Gaussian distribution

where

$$f(x) = \begin{cases} 1 & \text{for } |x| \leqslant a/2, \\ 0 & \text{for } |x| > a/2 \end{cases} \tag{26}$$

and

$$f(y) = \begin{cases} 1 & \text{for } |y| \leqslant b/2, \\ 0 & \text{for } |y| > b/2. \end{cases} \tag{27}$$

In this case the amplitude distribution of the acoustic potential in region (6) of the focal plane S_f has the following form

$$|\Phi(\xi, \eta)| = \frac{\varkappa_0}{2\pi f} |F(\xi)||F(\eta)|, \tag{28}$$

where

$$F(\xi) = a\,\mathrm{sinc}(av\xi/f) \tag{29}$$

and

$$F(\eta) = b\,\mathrm{sinc}(bv\eta/f), \tag{30}$$

while

$$\mathrm{sinc}(\alpha) = \mathrm{sinc}(\pi\alpha)/(\pi\alpha). \tag{31}$$

Let us analyse properties of this distribution along axis 0ξ. It has (Fig. 4) *a* main

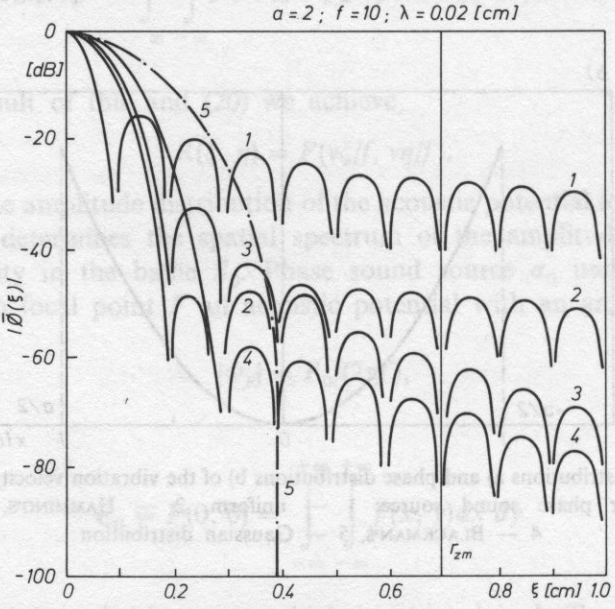

Fig. 4. Amplitude distribution of the acoustic potential in the focal point plane, produced by a rectangular focusing phase sound source with the following distributions: 1 — uniform, 2 — HAMMING'S, 3 — HANNING'S, 4 — BLACKMAN'S, 5 — GAUSSIAN

maximum in focal F equal to

$$|\Phi_F| = \varkappa_0 ab/(2\pi f) \tag{32}$$

and side maxima, which decrease with the increase of $|\xi|$ with the rate of 20 dB/decade. The width of the main maximum on level -3 dB is equal to

$$\Delta\xi = 0.9f/(av). \tag{33}$$

The highest side maximum is by 13 dB lower from the main maximum.

b) HAMMING'S distribution. It was assumed that the amplitude distribution of the vibration velocity in the baffle is determined by expression (Fig. 3)

$$f(x, y) = \varkappa_0 f(x) f(y), \tag{34}$$

where

$$f(x) = \begin{cases} 0.54 + 0.46\cos(2\pi x/a) & \text{for } |x| \leqslant a/2, \\ 0 & \text{for } |x| > a/2 \end{cases} \tag{35}$$

and

$$f(y) = \begin{cases} 0.54 + 0.46\cos(2\pi y/b) & \text{for } |y| \leqslant b/2, \\ 0 & \text{for } |y| > b/2. \end{cases} \tag{36}$$

In this case the amplitude distribution of the acoustic potential in the region (6) of the focal plane has the following form

$$|\Phi(\xi, \eta)| = \frac{\varkappa_0}{2\pi f} |F(\xi)||F(\eta)|, \tag{37}$$

$$F(\xi) = a[0.54\,\mathrm{sinc}(av\xi/f) + 0.23\,\mathrm{sinc}(av\xi/f - 1) + 0.23\,\mathrm{sinc}(av\xi/f + 1)] \tag{38}$$

and

$$F(\eta) = b[0.54\,\mathrm{sinc}(bv\eta/f) + 0.23\,\mathrm{sinc}(bv\eta/f - 1) + 0.23\,\mathrm{sinc}(bv\eta/f + 1)]. \tag{39}$$

This distribution has a main maximum in focal point F along the 0ξ axis (Fig. 4), equal to

$$|\Phi_F| = 0.54^2 \frac{\varkappa_0 ab}{2\pi f} \tag{40}$$

and side maxima, which decrease with the increase of $|\xi|$ with the rate of 20 dB/decade. The width of the main maximum on level -3 dB is equal to

$$\Delta\xi = 1.3f/(av). \tag{41}$$

The highest side maximum is by 42 dB lower than the main maximum.

c) HANNING'S distribution. Let us assume that the amplitude distribution of the vibration velocity in the baffle is determined as follows (Fig. 3)

$$f(x, y) = \varkappa_0 f(x) f(y), \tag{42}$$

where

$$f(x) = \begin{cases} 0.5 + 0.5\cos(2\pi x/a) & \text{for } |x| \leqslant a/2, \\ 0 & \text{for } |x| > a/2 \end{cases} \tag{43}$$

and

$$f(y) = \begin{cases} 0.5 + 0.5\cos(2\pi y/b) & \text{for } |y| \leqslant b/2, \\ 0 & \text{for } |y| > b/2. \end{cases} \tag{44}$$

In this case the amplitude distribution of the acoustic potential in region (6) of the focal plane has the following form

$$|\Phi(\xi, \eta)| = \frac{\varkappa_0}{2\pi f}|F(\xi)||F(\eta)|, \tag{45}$$

where

$$F(\xi) = a[0.5\,\mathrm{sinc}(av\xi/f) + 0.25\,\mathrm{sinc}(av\xi/f - 1) + 0.25\,\mathrm{sinc}(av\xi/f + 1)] \tag{46}$$

and

$$F(\eta) = b[0.5\,\mathrm{sinc}(bv\eta/f) + 0.25\,\mathrm{sinc}(bv\eta/f - 1) + 0.25\,\mathrm{sinc}(bv\eta/f + 1)]. \tag{47}$$

This distribution has a main maximum in focal point F along axis 0ξ (Fig. 4), equal to

$$|\Phi_F| = 0.5^2 \frac{\varkappa_0 ab}{2\pi f} \tag{48}$$

and side maxima, which decrease with the increase of $|\xi|$ with the rate of 60 dB/decade. The width of the main maximum on the level of -3 dB is equal to

$$\Delta\xi = 1.4f/(av). \tag{49}$$

The highest side maximum is by 32 dB smaller from the main maximum.

d) BLACKMAN'S distribution. Let us assume that the amplitude distribution of te vibration velocity in the baffle is determined as follows (Fig. 3)

$$f(x, y) = \varkappa_0 f(x) f(y), \tag{50}$$

where

$$f(x) = \begin{cases} 0.42 + 0.5\cos(2\pi x/a) + 0.08\cos(4\pi x/a) & \text{for } |x| \leqslant a/2, \\ 0 & \text{for } |x| > a/2 \end{cases} \tag{51}$$

and

$$f(y) = \begin{cases} 0.42 + 0.5\cos(2\pi x/b) + 0.08\cos(4\pi y/b) & \text{for } |y| \leqslant b/2, \\ 0 & \text{for } |y| > b/2. \end{cases} \tag{52}$$

In this case the amplitude distribution of the acoustic potential in region (6) of the focal plane has the following form

$$|\Phi(\xi, \eta)| = \frac{\varkappa_0}{2\pi f}|F(\xi)||F(\eta)|, \tag{53}$$

where

$$F(\xi) = a[0.42\,\mathrm{sinc}(av\xi/f) + 0.25\,\mathrm{sinc}(av\xi/f - 1) + 0.25\,\mathrm{sinc}(av\xi/f + 1) + \\ + 0.04\sin(av\xi/f - 2) + 0.04\sin(av\xi/f + 2)] \quad (54)$$

and

$$F(\eta) = b[0.42\,\mathrm{sinc}(bv\eta/f) + 0.25\,\mathrm{sinc}(bv\eta/f - 1) + 0.25\,\mathrm{sinc}(bv\eta/f + 1) + \\ + 0.04\,\mathrm{sinc}(bv\eta/f - 2) + 0.04\,\mathrm{sinc}(bv\eta/f + 2)]. \quad (55)$$

This distribution has a main maximum in focal point F along the 0ξ axis (Fig. 4), equal to

$$|\Phi_F| = 0.42^2 \frac{\varkappa_0 ab}{2\pi f} \quad (56)$$

and side maxima, which decrease with the increase of $|\xi|$ with the rate of 34 dB/decade. The width of the main maximum on the level of -3 dB is equals

$$\Delta\xi = 2f/(av). \quad (57)$$

The highest side maximum is by 57 dB lower from the main maximum.

e) Gaussian distribution. Let us assume that the amplitude distribution of the vibration velocity in the baffle is determined as follows (Fig. 3)

$$f(x, y) = \varkappa_0 f(x) f(y), \quad (58)$$

where

$$f(x) = \exp(-x^2/2\sigma_x^2) \quad (59)$$

and

$$f(y) = \exp(-y^2/2\sigma_y^2). \quad (60)$$

For comparison, Fig. 4 presents the amplitude distribution of the acoustic along the 0ξ axis, produced by a focusing rectangular phase source with a Gaussian amplitude distribution of the vibration velocity. It was accepted that $a = 7.06\sigma_x$ and $b = 7.06\sigma_y$. For these values of parameters σ_x and σ_y the Gaussian distribution assumes neglectable values along the edge of the source [11].

From among all analysed distributions, the main maximum of the amplitude distribution of the acoustic potential in region (6) of the focal plane S_f has the smallest width for the uniform distribution and the highest for BLACKMAN'S amplitude distribution of vibration velocity. The width of the main maximum for a given distribution increases with the increase of the focal lenght f of source σ_0 and with the increase of wave length λ, while it decreases with the increase of the a and b dimensions of the source. Side maxima are damped to the greatest extent for BLACKMAN'S distribution, and to the smallest extent for the uniform distribution. The

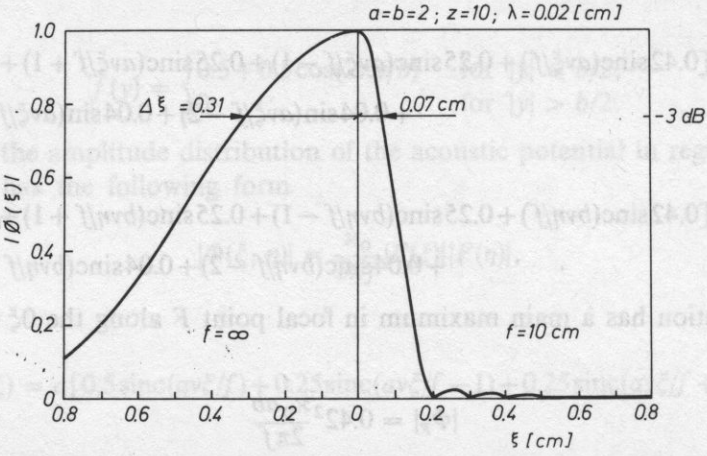

Fig. 5. A comparison between amplitude distribution of the acoustic potential at the same distance from a focusing and non-focusing rectangular sound source with HANNING'S amplitude distribution of the vibration velocity

HANNING'S distribution seems to be of greatest practical application. It makes it possible to locate sources in casings along its edge. For this amplitude distribution of vibration velocity, the amplitude distribution of the acoustic potential in the focal plane S_f has a relatively narrow main maximum and sufficiently strongly damped side maxima. For comarative reasons amplitude distributions of the acoustic potential produced in region (6) of the same plane S_z by a focusing and non-focusing rectangular sound with HANNING'S amplitude distribution of vibration velocity have been presented in Fig. 5.

5. Amplitude distribution of the acoustic potential along the main axis

Let us determine the amplitude distribution of the acoustic potential along the main axis $0z$ of a focusing rectangular phase source σ_0. Accepting in (14) that $\xi, \eta = 0$ we obtain

$$|\Phi(z)| = \frac{1}{2\pi z}|R(z)|, \tag{61}$$

where

$$R(z) = \int_{-a/2}^{+a/2}\int_{-b/2}^{+b/2} f(x, y)\exp\left[-j\frac{\pi\nu}{w}(x^2+y^2)\right]dxdy. \tag{62}$$

Amplitude distributions of the acoustic potential along the main axis of a focusing square phase source σ_0 with the following distributions of the amplitude of vibration velocity: uniform, HAMMING'S, HANNING'S and BLACKMAN'S were

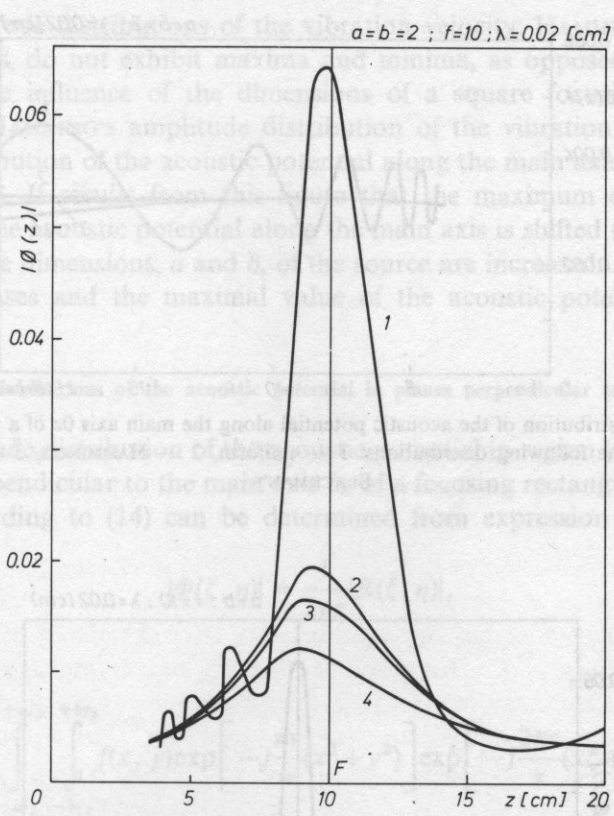

Fig. 6. Amplitude distributions of the acoustic potential along the main axis $0z$ of a focusing square phase sound source with the following distributions: 1 — uniform, 2 — HAMMING'S, 3 — HANNING'S, 4 — BLACKMAN'S

calculated on a minicomputer with the application of the trapezoid method of calculating the values of definite integrals. Results are presented in Fig. 6. It can be seen that at a uniform amplitude distribution of vibration velocity, the amplitude distribution of the acoustic potential along the $0z$ axis has a main maximum located at a small distance before the focal point F and is preceeded by a series of initial maxima and minima. As for HAMMING'S, HANNING'S and BLACKMAN'S distributions, the amplitude distribution of the acoustic potential along the main axis $0z$ has only one maximum shifted slightly further towards the source. The amplitude of the acoustic potential in this maximum acquires the highest value for HAMMING'S distribution and the lowest value for BLACKMAN'S distribution. The main maximum is shifted towards the source the most for BLACKMAN'S distribution. For comparison, Fig. 7 presents amplitude distributions of the acoustic potential along the main axis $0z$ for a non-focusing square sound source with the following amplitude distribution of the vibration velocity: uniform, HAMMING'S, HANNING'S and BLACKMAN'S. In this case amplitude distributions of the acoustic potential along the main axis for the

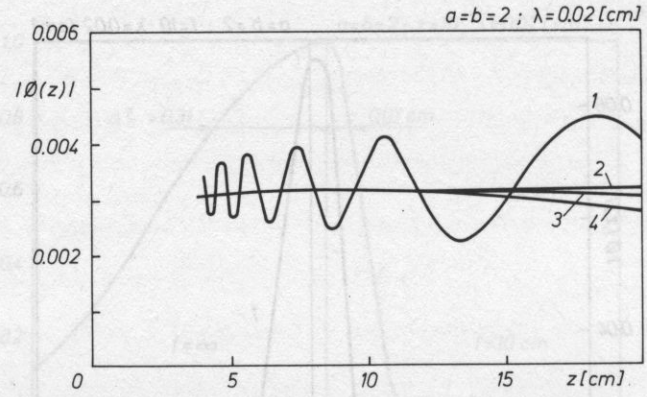

Fig. 7. Amplitude distribution of the acoustic potential along the main axis 0z of a non-focusing square sound source with the following distributions: 1 — uniform, 2 — HAMMING'S, 3 — HANNING'S, 4 — BLACKMAN'S

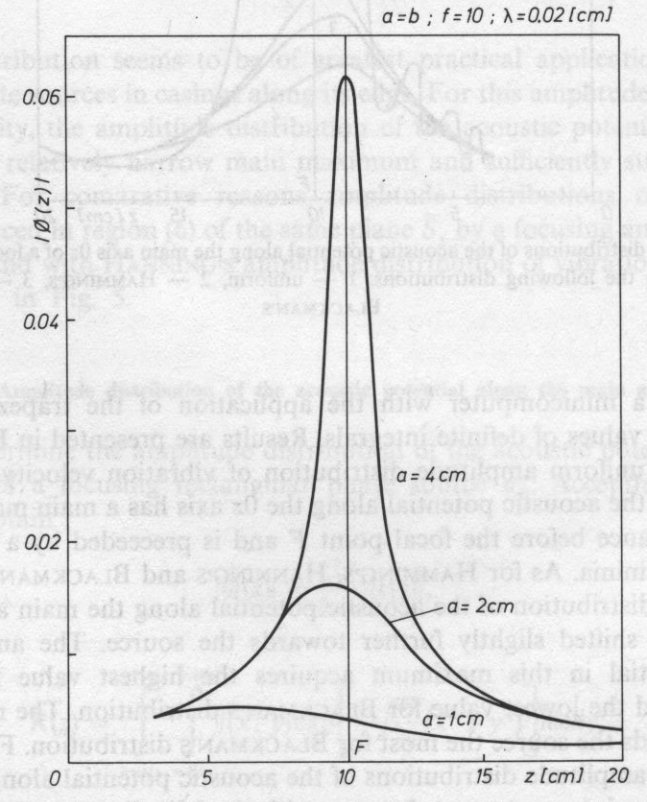

Fig. 8. The influence of dimensions of a focusing square phase sound source with HAMMING'S amplitude distribution of vibration velocity on the amplitude distribution of the acoustic potential along the main axis 0z

following amplitude distributions of the vibration velocity: HAMMING'S, HANNING'S and BLACKMAN'S, do not exhibit maxima and minima, as opposed to the uniform distribution. The influence of the dimensions of a square focusing phase sound source with a HANNING'S amplitude distribution of the vibration velocity, on the amplitude distribution of the acoustic potential along the main axis of this source is shown in Fig. 8. It results from this figure that the maximum of the amplitude distribution of the acoustic potential along the main axis is shifted towards the focal point F when the dimensions, a and b, of the source are increased. At the same time its width decreases and the maximal value of the acoustic potential increases.

6. Amplitude distributions of the acoustic potential in planes perpendicular to the main axis

The amplitude distribution of the acoustic potential in region (6) of an arbitrary plane $z \neq f$, perpendicular to the main axis $0z$ of a focusing rectangular phase sound source σ_0 according to (14) can be determined from expression

$$|\Phi(\xi, \eta)| = \frac{1}{2\pi z}|R(\xi, \eta)|, \tag{63}$$

where

$$R(\xi, \eta) = \int_{-a/2}^{+a/2}\int_{-b/2}^{+b/2} f(x, y)\exp\left[-j\frac{\pi v}{w}(x^2+y^2)\right]\exp\left[-j\frac{2\pi v}{z}(x\xi+\eta)\right]dxdy. \tag{64}$$

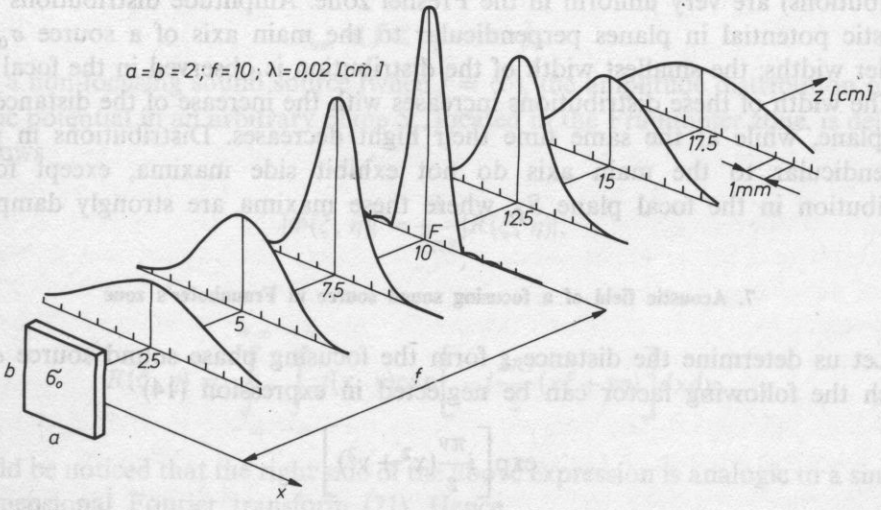

Fig. 9. Amplitude distributions of the acoustic potential at various distances from a focusing square phase sound source with a HANNING'S amplitude distribution of vibration velocity

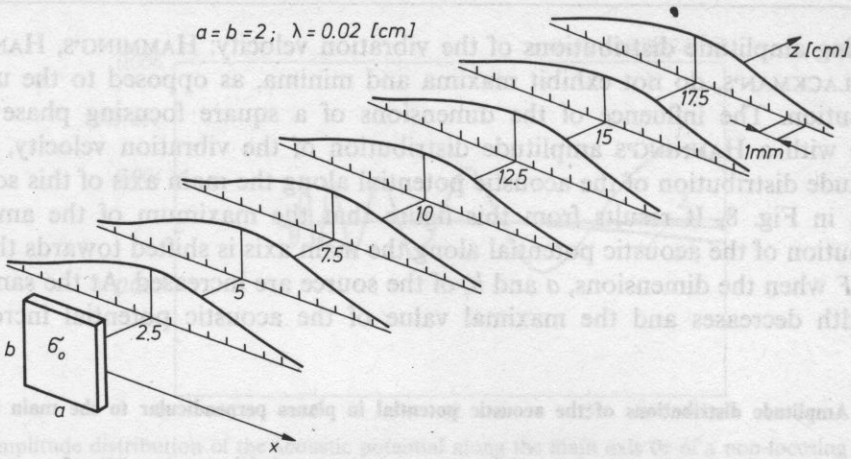

Fig. 10. Amplitude distributions of the acoustic potential at various distances from a non-focusing square source with HANNING'S amplitude distribution of vibration velocity

The amplitude distribution of the acoustic potential in chosen planes perpendicular to the main axis of a focusing square phase sound source with a HANNING'S amplitude distribution of the vibration velocity were calculated by a minicomputer with the application of the trapezoid method of calculating the value of definite integrals. Results are presented in Fig. 9. For comparison, Fig. 10 presents amplitude distributions of the acoustic potential in the same planes for a non-focusing square sound source with the same dimensions and with a HANNING'S amplitude distribution of vibration velocity. It results from the figure that acoustic fields of a focusing and non-focusing square sound source with a HANNING'S amplitude distribution of vibration velocity (as well as with the HAMMING'S and BLACKMAN'S distributions) are very uniform in the Fresnel zone. Amplitude distributions of the acoustic potential in planes perpendicular to the main axis of a source σ_0 have smaller widths; the smallest width of the distribution is observed in the focal plane S_f. The width of these distributions increases with the increase of the distance from this plane, while at the same time their hight decreases. Distributions in planes perpendicular to the main axis do not exhibit side maxima, except for the distribution in the focal plane S_f, where these maxima are strongly damped.

7. Acoustic field of a focusing sound source in Fraunhofer's zone

Let us determine the distance z form the focusing phase sound source σ_0, for which the following factor can be neglected in expression (14)

$$\exp\left[j\frac{\pi v}{z}(x^2+y^2)\right]. \tag{65}$$

It was assumed that this is possible, if the phase of this factor will change more less

than one radian in the region of the source σ_0. Because

$$x^2+y^2 \leqslant r_{om}^2, \tag{66}$$

where r_{om} is the greatest distance between the points of the contour of the source and the origin of coordinates (Fig. 1); then factor (65) can be neglected when

$$\pi v r_{om}^2/z \ll 1. \tag{67}$$

Hence, at a distance from source σ_0 we have

$$z \gg z_g = \pi v r_{om}^2, \tag{68}$$

i.e. [4, 10], when the plane S_z is located in the Fraunhofer zone of this source. According to this and (14) the amplitude distribution of the acoustic potential in plane S_z, which is located in the far field of a focusing phase sound source σ_0, can be defined as

$$|\Phi(\xi, \eta)| = \frac{1}{2\pi z}|R(\xi, \eta)|, \tag{69}$$

where

$$R(\xi, \eta) = \int_{-\infty}^{+\infty}\int_{-\infty}^{+\infty} f(x, y)\exp\left[-j\frac{\pi v}{f}(x^2+y^2)\right]\exp\left[-j\frac{2\pi v}{z}(x\xi+y\eta)\right]dxdy. \tag{70}$$

It results from this and (20) that the energy of vibrations radiated by a focusing phase source σ_0 can not be focused in the Fraunhofer zone. Therefore, the focal point F has to be located in the Fresnel zone of the source σ_0, i.e. its focal length has to satisfy the condition

$$r_{om} \ll f \leqslant z_g = \pi v r_{om}^2. \tag{71}$$

As for a non-focusing sound source (when $f = \infty$), the amplitude distribution of the acoustic potential in an arbitrary plane S_z, located in the Fraunhofer zone, is defined as follows

$$|\Phi(\xi, \eta)| = \frac{1}{2\pi z}|R(\xi, \eta)|, \tag{72}$$

where

$$R(\xi, \eta) = \int_{-\infty}^{+\infty}\int_{-\infty}^{+\infty} f(x, y)\exp\left[-j\frac{2\pi v}{z}(x\xi+y\eta)\right]dxdy. \tag{73}$$

It should be noticed that the right side of the above expression is analogic to a simple two-dimensional Fourier transform (21). Hence,

$$R(\xi, \eta) = F(v\xi/z, v\eta/z). \tag{74}$$

Therefore, the amplitude distribution of the acoustic potential in region (6) of an arbitrary plane S_z, located in the Fraunhofer zone of a non-focusing sound source σ_0, is defined by the spatial spectrum of the amplitude distribution of the vibration velocity in the baffle S_0, produced by this source. Focusing properties of a source become negligible with the increase of the distance from the source; the complex character of radiation of the source vanishes and the field produced by it becomes more similar to the field produced by plane sound wave.

8. Conclusions

On the basis of the above discussion, it can be stated that in the Fresnel zone acoustic fields of focusing and non-focusing rectangular sound sources with the amplitude distributions of vibration velocity: HAMMING'S, HANNING'S and BLACKMAN'S, are very uniform, very much like acoustic fields in this zone of focusing and non-focusing circular sound sources with Gaussian amplitude distributions of vibration velocity [2, 3]. Amplitude distributions of the acoustic potential along the main axis of a focusing rectangular phase sound source with HAMMING'S, HANNING'S and BLACKMAN'S amplitude distributions of vibration velocity, have only one maximum located near the focal point. This maximum has the greatest value in the case of HAMMING'S distribution. The value of the maximum increases and is shifted towards the focal point when the dimensions of the source are increased. Maxima of amplitude distributions of the acoustic potential in planes perpendicular to the main axis of a focusing and non-focusing rectangular sound source are located along this axis and in the Fresnel zone of a focusing sound source these maxima are much narrower. The main maximum in the focal plane has the smallest width and the highest value. This maximum is accompanied by side maxima, strongly damped in the case of HAMMING'S, HANNING'S and BLACKMAN'S distribution. From among all analysed distributions, the width of the main maximum was smallest for the uniform distribution and largest for BLACKMAN'S distribution. However, they are much more narrow than the width of the main maximum of the amplitude distribution of the acoustic potential in the focal plane, produced by a focusing sound source with a Gaussian amplitude distribution of the vibration velocity. It seems possible to use a focusing square phase sound source with adequately great dimensions with respect to the wave length (e.g. $a/\lambda = 200$) and HANNING'S amplitude distribution of the vibration velocity, in ultrasonic diagnostic systems in order to increase their transverse resolving power. Such a source can be realized in practice in the form of a phase system of piezoelectric transducers with a discrete HANNING'S distribution of their bulk efficiencies. The desired efficiency distribution of individual transducers and adequate phases of vibrations can be obtained by a suitable selection of amplitudes and reciprocal phase shifts of input signals. Yet a more detailed analysis of this problem requires a separate paper.

References

[1] W. T. CATHEY, *Optical information processing and holography*, John Wiley and Sons, New York 1974.

[2] L. FILIPCZYŃSKI, J. ETIENNE, *Theory and experimental research of spherical focusing transducers with Gaussian surface velocity distribution*, Archiwum Akustyki, **8**, 4, 341–360 (1973) (in Polish).

[3] K. V. HASELBERG, J. KRAUTKRÄMER, *Ein Ultraschall-Strahler für die Werkstoffprüfung mit verbessertem Nahfeld*, Acustica, **9**, 5, 359–364 (1959).

[4] L. E. KINSLER, A. R. FREY' A. B. COOPENS, J. V. SANDERS, *Fundamentals of acoustics*, John Wiley and Sons, New York 1982.

[5] T. KUJAWSKA, *Dynamic focusing of an ultrasonic beam with a phase system of annular transducers with the application of the pulse technique*, Archiwum Akustyki, **18**, 1, 71–83 (1983) (in Polish).

[6] F. MARZIN, M. BREAZEALE, *A simple way to eliminate diffraction lobes emitted by ultrasonic transducers*, Journ. Acoust. Soc. Am., **49**, 5 (Part 2), 1668–1669 (1971).

[7] H. T. O'NEIL, *Theory of focusing radiators*, Journ. Acoust. Soc. Am., **21**, 5, 318–526 (1949).

[8] W. PAJEWSKI, *Piezoelectric transducers for ultrasonic energy concentration*, Archiwum Akustyki, **5**, 4, 421 (1970) (in Polish).

[9] A. PUCH, *Rectangular sources and systems of sound sources with large directionality*, Archives of Acoustics, **10**, 1, 17–35 (1985).

[10] W. RDZANEK, *Theory of the acoustic field. Chosen problems*, WSP, Zielona Góra 1982 (in Polish).

[11] J. SZABATIN, *Fundamentals of the theory of signals*, WKŁ, Warszawa 1982 (in Polish).

[12] T. WASZCZUK, T. KUJAWSKA, J. C. SOMER, *Ultrasonic beam focusing with a piezoelectric multi-annular transducer*, Archiwum Akustyki, **18**, 3, 201–221 (1983) (in Polish).

Received on June 26, 1985; revised version on July 25, 1986.

ARCHIVES OF ACOUSTICS
12, 1, 53–69 (1987)

ENERGETIC PROPERTIES OF RECTANGULAR SOUND SOURCES WITH LARGE DIRECTIONALITY

ANDRZEJ PUCH

Institute of Physics, Higher Pedagogical School in Rzeszów
(35–310 Rzeszów, ul. Rejtana 16a)

In this paper the author investigated energetic properties of rectangular sound sources with the following amplitude distributions of the vibration velocity: uniform, HAMMING'S, HANNING'S and BLACKMAN'S. The frequency characteristics of the active power, reactive power and apparent power of these sources was determined, as well as their power factor. It was found that sources under investigations effectively radiate vibration energy into the far field (i.e. with the power factor equal to one) in the wave length range, in which they exhibit large directionality. The energy of vibrations radiated by a source into the far field in a unit of time is by an order of magnitude smaller in the case of HAMMING'S, HANNING'S and BLACKMAN'S distributions than in the case of a uniform distribution. Therefore, an increase of the directivity of radiation of the vibration energy into the far field by rectangular sound sources is accompanied by a decrease of the value of radiated energy.

1. Introduction

There is a need for sound sources with large directionality of vibration energy radiated into the far field in many domains: metrology, diagnostics, hydrolocation and ultrasonic technology. They are applied to obtain an adequate beam of ultrasonic waves or to obtain a required concentration of energy in a certain area of the medium. In these applications sound sources have to radiate energy of vibrations effectively. The far field of a rectangular sound source with uniform, HANNING'S and BLACKMAN'S amplitude distributions of the vibration velocity have been investigated in paper [5]. It was stated that the directional characteristic of such a source with HANNING'S distribution has a relatively narrow main maximum (much more narrow than for a Gaussian distribution [10]) and sufficiently strongly damped side maxima. It was also found that a sound source, which radiates energy of vibrations into the far field with a sufficiently large directionality, can be in practice realized by a mosaic system of plane sound sources with discrete HANNING'S distributions of their

relative bulk efficiencies. This paper analyses energetic properties of rectangular sound sources with large directionality of energy radiate into the far field. A developed by the author new method of determining frequency characteristics of the reactive power of sound sources with the application of a fast Fourier transform was used in investigations.

2. Acoustic field of plane sound sources

Let us accept (Fig. 1) that a plane sound source σ_0, which vibrates with a simple periodic motion with frequency f_0, is situated in plane $z = 0$, which is a perfectly rigid baffle S_0. It was also assumed that the distribution of the normal component of the amplitude of vibration velocity produced by source σ_0 in the baffle S_0 is defined by the following function

$$\begin{aligned} &\varkappa(x_0, y_0) \neq 0 \quad \text{for surface of the source } \sigma_0; \\ &\varkappa(x_0, y_0) = 0 \quad \text{for the rest of the surface of the baffle } S_0. \end{aligned} \tag{1}$$

Let us assume that source σ_0 radiates the energy of vibrations into the half-space $z > 0$ filled with a lossless and homogeneous fluid medium with density ϱ, in which a sound wave propagates with velocity c. The amplitude distribution of the acoustic potential in this half-space is determined by the solution of Helmholtz's equation [2, 6]

$$\Delta\Phi(x, y, z) + 4\pi^2 \nu^2 \Phi(x, y, z) = 0 \tag{2}$$

which satisfies Neumann's boundary condition

$$\frac{\partial}{\partial z}\Phi(x, y, z)\bigg|_{z=0} = -\varkappa(x_0, y_0) \tag{3}$$

and Sommerfeld's condition of finity

$$\lim_{r \to \infty} \Phi(x, y, z) = 0 \tag{4}$$

and radiation

$$\lim_{r \to \infty} r\left[\frac{\partial}{\partial r}\Phi(x, y, z) + j2\pi\nu\Phi(x, y, z)\right] = 0 \tag{5}$$

where Δ is a Laplacian, $\nu = f_0/c$ — spatial frequency of a sound wave with frequency f_0, which propagates with velocity c in the direction of radius r (Fig. 1).

Let us consider an arbitrary plane S_z, situated in half-space $z > 0$ and parallel to the baffle S_0 (Fig. 1). The distance between these two planes is denoted by z. Function $\Phi(x, y, z)$ defines the amplitude distribution of the acoustic potential produced by source σ_0 in plane S_z. Now we will define components of the spatial frequency of a plane sound wave propagating in the direction of radius r:

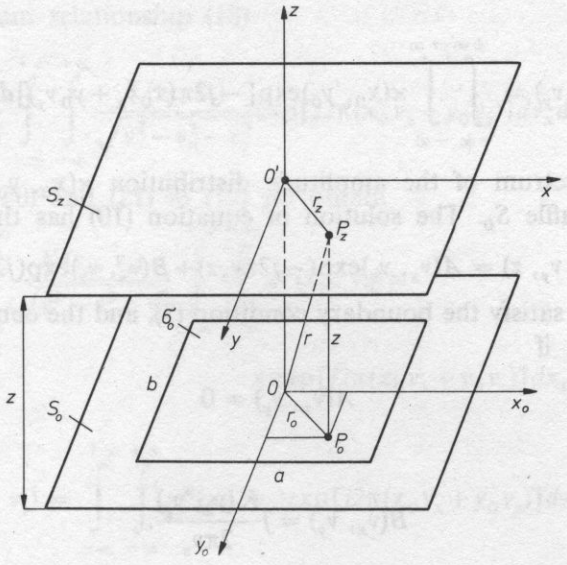

Fig. 1. Plane sound source σ_0 located in baffle S_0, which radiates energy of vibrations into a medium, which fills the half-space above the baffle

$$v_x = v\cos(x, r), \tag{6}$$

$$v_y = v\cos(y, r), \tag{7}$$

$$v_z = v\cos(z, r). \tag{8}$$

The spatial spectrum of the amplitude distribution of the acoustic potential in plane S_z is determined with the application of a simple two-dimensional Fourier transform [1]. Namely,

$$F(v_x, v_y\, z) = \int_{-\infty}^{+\infty}\int_{-\infty}^{+\infty} \Phi(x, y, z)\exp[-j2\pi(xv_x + yv_y)]dxdy. \tag{9}$$

In accordance to this, equation (2) and the boundary condition (3) can be written as follows

$$\frac{d^2}{dz^2}F(v_x, v_y, z) + 4\pi^2 v_z^2 F(v_x, v_y, z) = 0, \tag{10}$$

where

$$v_z = \sqrt{v^2 - v_x^2 - v_y^2} \tag{11}$$

and

$$\frac{d}{dz}F(v_x, v_y, z)\Big|_{z=0} = -K(v_x, v_y), \tag{12}$$

while

$$K(v_x, v_y) = \int_{-\infty}^{+\infty}\int_{-\infty}^{+\infty} \varkappa(x_0, y_0)\exp[-j2\pi(x_0 v_x + y_0 v_y)]dx_0 dy_0 \tag{13}$$

is the spatial spectrum of the amplitude distribution $\varkappa(x_0, y_0)$ of the vibration velocity in the baffle S_0. The solution of equation (10) has the following from

$$F(v_x, v_y, z) = A(v_x, v_y)\exp(-j2\pi v_z z) + B(v_x, v_y)\exp(j2\pi v_z z). \tag{14}$$

This solution will satisfy the boundary condition (3), and the conditions of finity (4) and radiation (5), if

$$A(v_x, v_y) = 0 \tag{15}$$

and

$$B(v_x, v_y) = j\frac{K(v_x, v_y)}{2\pi v_z}. \tag{16}$$

Hence the solution of (14) has the following form

$$F(v_x, v_y, z) = jK(v_x, v_y)\frac{\exp(j2\pi v_z z)}{2\pi v_z}. \tag{17}$$

With the application of the inverse Fourier transform [1], we can determine the interesting to us amplitude distribution of the acoustic potential in an arbitrary plane S_z, parallel to the baffle S_0 on the basis of dependence (17). Namely

$$\Phi(x, y, z) = j\int_{-\infty}^{+\infty}\int_{-\infty}^{+\infty} K(v_x, v_y)\frac{\exp(j2\pi v_z z)}{2\pi v_z}[j2\pi(xv_x + yv_y)]dv_x dv_y. \tag{18}$$

3. Sound power of a plane source

The sound power of a plane source σ_0, situated in baffle S_0 can be derived from [2, 6]

$$N = (1/2)\int_{-\infty}^{+\infty}\int_{-\infty}^{+\infty} \varkappa^*(x_0, y_0)P(x_0, y_0)dx_0 dy_0, \tag{19}$$

where function $\varkappa^*(x, y)$ denotes the distribution of the complex conjugate amplitude of the vibration velocity in the baffle S_0 and function $P(x, y)$ determines the amplitude distribution of the acoustic pressure in this plane. Because [2]

$$P(x_0, y_0) = -j2\pi\nu\varrho c\Phi(x_0, y_0), \tag{20}$$

while for $z = 0$ from relationship (18)

$$\Phi(x_0, y_0) = j\frac{1}{2\pi}\int_{-\infty}^{+\infty}\int_{-\infty}^{+\infty}\frac{K(v_x, v_y)}{\sqrt{v^2 - v_x^2 - v_y^2}}\exp[j2\pi(x_0 v_x + y_0 v_y)]dv_x dv_y \tag{21}$$

thus substituting (20) and (21) in (19) we obtain

$$N = \frac{v\varrho c}{2}\int_{-\infty}^{+\infty}\int_{-\infty}^{+\infty}\frac{K(v_x, v_y)}{\sqrt{v^2 - v_x^2 - v_y^2}}\int_{-\infty}^{+\infty}\int_{-\infty}^{+\infty}\varkappa^*(x_0, y_0)\times$$

$$\times\exp[j2\pi(x_0 v_x + y_0 v_y)]dx_0 dy_0 dv_x dv_y. \tag{22}$$

For [1]

$$K^*(v_x, v_y) = \int_{-\infty}^{+\infty}\int_{-\infty}^{+\infty}\varkappa^*(x_0, y_0)\exp[j2\pi(x_0 v_x + y_0 v_y)]dx_0 dy_0 \tag{23}$$

is the complex conjugate spatial spectrum of the amplitude distribution of the vibration velocity in the baffle S_0, thus

$$N = \frac{v\varrho c}{2}\int_{-\infty}^{+\infty}\int_{-\infty}^{+\infty}\frac{|K(v_x, v_y)|^2}{\sqrt{v^2 - v_x^2 - v_y^2}}dv_x dv_y. \tag{24}$$

It results from this relationship that the acoustic power of a plane sound source σ_0 is a complex quantity. Let

$$N = N_R + jN_I, \tag{25}$$

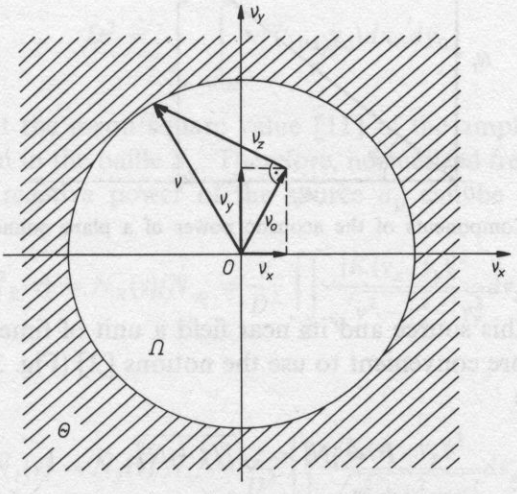

Fig. 2. Integration regions in the determination of the active and reactive power of a plane sound source

where N_R is the active power and N_I is the reactive power of such a source. We will consider the plane of components v_x and v_y of spatial frequency (Fig. 2). It results from (24) that the active power of the sound source σ_0 can be determined from relationship

$$N_R = \frac{v\varrho c}{2} \iint\limits_{\Omega} \frac{|K(v_x, v_y)|^2}{\sqrt{v^2 - v_x^2 - v_y^2}} dv_x dv_y \tag{26}$$

by integrating in the region Ω, of spatial components v_x and v_y, in which

$$v_x^2 + v_y^2 \leqslant v^2. \tag{27}$$

Whereas the reactive power of this source can be determined from

$$N_I = -\frac{v\varrho c}{2} \iint\limits_{\theta} \frac{|K(v_x, v_y)|^2}{\sqrt{v_x^2 + v_y^2 - v^2}} dv_x dv_y, \tag{28}$$

where the integration in done in the region θ of spatial frequencies v_x and v_y, in which

$$v_x^2 + v_y^2 > v^2. \tag{29}$$

The active power of source σ_0 determines its energy of vibrations, which is radiated in a unit of time into the far field, while the reactive power determines the energy

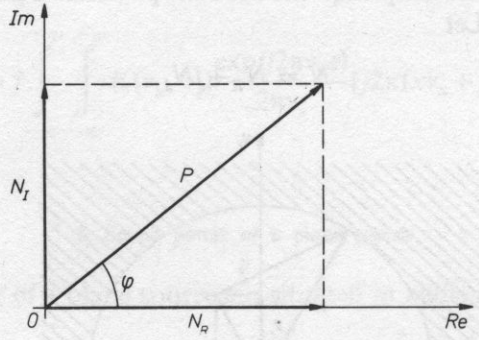

Fig. 3. Components of the acoustic power of a plane sound source

exchanged between this source and its near field a unit of time. From the practical point of view it is more convenient to use the notions [2] (Fig. 3) of apparent power of the sound source

$$P = |N| = \sqrt{N_R^2 + N_I^2}, \tag{30}$$

which determines the total acoustic energy of the source related to a unit of time, and

power factor

$$\cos\varphi = N_R/P, \tag{31}$$

which informs what part of this energy is radiated by the source into the far field in a unit of time.

4. Energetic characteristics of a sound source

It should be noticed that the acoustic power of the sound source σ_0 (and hence its active power, reactive power, apparent power and power factor) depend on the vibration frequency f_0 of its surface through the spatial frequency v. Functions presenting the relationship between the spatial frequency v and these quantities are called energetic characteristics of sound source σ_0 [2]. It is more convenient to use normalized energetic characteristics when comparing energetic properties of sound source. We have

$$\lim_{v\to\infty} N(v) = \frac{\varrho c}{2} D^2 = N_\infty, \tag{32}$$

where

$$D^2 = \int_{-\infty}^{+\infty}\int_{-\infty}^{+\infty} |K(v_x, v_y)|^2 dv_x dv_y. \tag{33}$$

With the application of Parseval's theorem [1] the above expression can be written as

$$D^2 = \int_{-\infty}^{+\infty}\int_{-\infty}^{+\infty} \varkappa^2(x_0, y_0) dx_0 dy_0. \tag{34}$$

It results that D^2 it the meon square value [11] of the amplitude of the vibration velocity distribution in the baffle S_0. Therefore, normalized frequency characteristics of the active and reactive power of the source σ_0 can be defined as

$$\bar{N}_R(v) = N_R(v)/N_\infty = \frac{v}{D^2}\iint_\Omega \frac{|K(v_x, v_y)|^2}{\sqrt{v^2 - v_x^2 - v_y^2}} dv_x dv_y, \tag{35}$$

where as

$$\bar{N}_I(v) = N_I(v)/N_\infty = \frac{v}{D^2}\iint_\theta \frac{|K(v_x, v_y)|^2}{\sqrt{v_x^2 + v_y^2 - v^2}} dv_x dv_y, \tag{36}$$

while

$$\lim_{\nu \to \infty} \bar{N}_R(\nu) = 1 \tag{37}$$

and

$$\lim_{\nu \to \infty} \bar{N}_I(\nu) = 0. \tag{38}$$

5. Methods of determining energetic characteristics of sound sources

Energetic characteristics of sound sources are most frequently determined directly form relationships (35), (36) and (30), (31) (e.g. [6, 7]). It was proved in papers [9] and [10] that the characteristics of the reactive power of a sound source can be determined on the basis of its frequency characteristic of the active power, with the application of a simple Hilbert transformation. Namely,

$$\bar{N}_I(\nu) = \frac{1}{\pi\nu} * \bar{N}_R(\nu) = \frac{1}{\pi} \int_{-\infty}^{+\infty} \frac{\bar{N}_R(\eta)}{\nu - \eta} d\eta. \tag{39}$$

Now we will prove that the frequency characteristic of the reactive power of a sound source can be determined on the basis of its frequency characteristic of the active power, with the application of a simple and inverse Fourier transform. Fourier transform of both sides of the relationship (39) were determined. Taking advantage [11] of the theorem about the Fourier transform of a convolution and the theorem about the Fourier transform of function $1/(\pi\nu)$ we obtain

$$\bar{\mathcal{N}}_{I\mu} = -j\,\mathrm{sgn}(\mu)\bar{\mathcal{N}}_R(\mu), \tag{40}$$

where distribution

$$\mathrm{sgn}(\mu) = \begin{cases} 1 & \text{for } \mu > 0, \\ 0 & \text{for } \mu = 0, \\ -1 & \text{for } \mu < 0. \end{cases} \tag{41}$$

Hence, on the basis of the inverse Fourier transform [11] we can note

$$\bar{N}_I(\nu) = \int_{-\infty}^{+\infty} \bar{\mathcal{N}}_I(\mu)\exp(j2\pi\nu\mu)d\mu, \tag{42}$$

where

$$\bar{\mathcal{N}}_I(\mu) = -j\,\mathrm{sgn}(\mu)\bar{\mathcal{N}}_R(\mu), \tag{43}$$

while

$$\bar{\mathcal{N}}_R(\mu) = \int_{-\infty}^{+\infty} \bar{N}(v)\exp(-j2\pi\mu v)dv. \tag{44}$$

The resulting from above considerations algorithm of determining the frequency characteristic of the reactive power of a sound source on the basis of its frequency characteristic of the active power with the application of the Fourier transform is presented in Fig. 4.

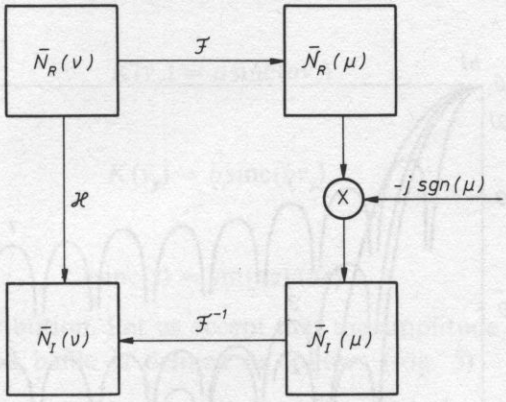

Fig. 4. Algorithms of determining the frequency characteristic of the reactive power of a sound source: $\mathcal{H}$ — Hilbert's transform, $\mathcal{F}$ — Fourier transform, $\mathcal{F}^{-1}$ — inverse Fourier transform

The frequency characteristics of the active power of sound sources with large directionality have been determined in this paper from relationship (35) with the application of the trapezoid method of calculating the values of definite integrals. While frequency characteristics of the reactive power of these sources were determined in accordance with the algorithm presented in Fig. 4 with the application of a simple and inverse discrete Fourier transform [3, 4]. The Cooley-Tukey algorithm of the fast Fourier transform [3, 4] was used in the course of calculations. Calculations were performed on a minicomputer.

6. Rectangular sound sources with large directionality

Let us accept that a sound source σ_0 has a shape of a rectangular with sides a and b (Fig. 1). We will analyse the following amplitude distributions of the vibration velocity in the baffle S_0: uniform, HAMMING'S, HANNING'S and BLACKMAN'S. It was proved in paper [5] that for HAMMING'S, HANNING'S and BLACKMAN'S distributions, the directional characteristic of a rectangular sound has a relatively narrow main

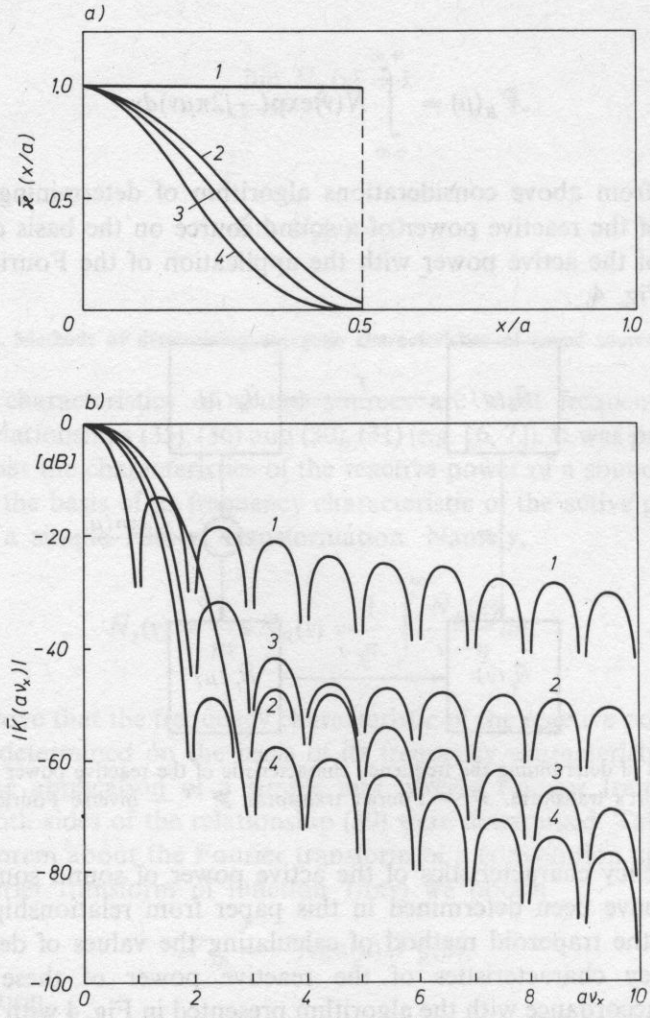

Fig. 5. Amplitude distributions of the vibration velocity on the surface of a rectangular sound source a) and their spatial spectra b): 1 — uniform, 2 — HAMMING'S, 3 — HANNING'S, 4 — BLACKMAN'S distribution

maximum and sufficiently strongly damped side maxima, if the dimensions of the source are sufficiently large in relation to the wave length.

a) Uniform distribution. Let us accept that the amplitude distribution in the baffle S_0 is determined as follows (Fig. 5)

$$\varkappa(x_0, y_0) = \varkappa_0 \varkappa(x_0) \varkappa(y_0), \tag{45}$$

where

$$\varkappa(x_0) = \begin{cases} 1 & \text{for } |x_0| \leqslant a/2, \\ 0 & \text{for } |x_0| > a/2 \end{cases} \tag{46}$$

and

$$\varkappa(y_0) = \begin{cases} 1 & \text{for } |y_0| \leqslant b/2, \\ 0 & \text{for } |y_0| > b/2. \end{cases} \tag{47}$$

The mean square value of this distribution is equal to

$$D^2 = \varkappa_0^2 ab, \tag{48}$$

while its spatial spectrum (Fig. 5) is given as

$$K(v_x, v_y) = \varkappa_0 K(v_x) K(v_y), \tag{49}$$

where

$$K(v_x) = a\,\mathrm{sinc}(av_x) \tag{50}$$

and

$$K(v_y) = b\,\mathrm{sinc}(bv_y), \tag{51}$$

while

$$\mathrm{sinc}(z) = \sin(\pi z)/(\pi z). \tag{52}$$

b) HAMMING'S distribution. Let us accept that the amplitude distribution of the vibration velocity in the baffle is defined as follows (Fig. 5)

$$\varkappa(x_0, y_0) = \varkappa_0 \varkappa(x_0) \varkappa(y_0), \tag{53}$$

where

$$\varkappa(x_0) = \begin{cases} 0.54 + 0.46\cos(2\pi x_0/a) & \text{for } |x_0| \leqslant a/2, \\ 0 & \text{for } |x_0| > a/2 \end{cases} \tag{54}$$

and

$$\varkappa(y_0) = \begin{cases} 0.54 + 0.46\cos(2\pi y_0/b) & \text{for } |y_0| \leqslant b/2, \\ 0 & \text{for } |y_0| > b/2. \end{cases} \tag{55}$$

The mean square value of this distribution is equal to

$$D^2 = 0.158\varkappa^2 ab, \tag{56}$$

while its spatial spectrum (Fig. 5) is given as

$$K(v_x, v_y) = \varkappa_0 K(v_x) K(v_y), \tag{57}$$

where

$$K(v_x) = a[0.54\,\mathrm{sinc}(av_x) + 0.23\,\mathrm{sinc}(av_x - 1) + 0.23\,\mathrm{sinc}(av_x + 1)] \tag{58}$$

and

$$K(v_y) = b[0.54\,\mathrm{sinc}(bv_y) + 0.23\,\mathrm{sinc}(bv_y - 1) + 0.23\,\mathrm{sinc}(bv_y + 1)]. \tag{59}$$

c) HANNING'S distribution. Let us accept that the amplitude distribution of the vibration velocity in the baffle is defined as follows (Fig. 5)

$$\varkappa(x_0, y_0) = \varkappa_0 \varkappa(x_0)\varkappa(y_0), \tag{60}$$

where

$$\varkappa(x_0) = \begin{cases} 0.5+0.5\cos(2\pi x_0/a) & \text{for } |x_0| \leqslant a/2, \\ 0 & \text{for } |x_0| > a/2 \end{cases} \tag{61}$$

and

$$\varkappa(y_0) = \begin{cases} 0.5+0.5\cos(2\pi y_0/b) & \text{for } |y_0| \leqslant b/2, \\ 0 & \text{for } |y_0| > b/2. \end{cases} \tag{62}$$

The mean square value of this distribution is equal to

$$D^2 = 0.141\varkappa_0^2 ab, \tag{63}$$

while its spatial spectrum (Fig. 5) is given as

$$K(v_x, v_y) = \varkappa_0 K(v_x)K(v_y), \tag{64}$$

where

$$K(v_x) = a[0.5\,\mathrm{sinc}(av_x)+0.25\,\mathrm{sinc}(av_x-1)+0.25\,\mathrm{sinc}(av_x+1)] \tag{65}$$

and

$$K(v_y) = b[0.5\,\mathrm{sinc}(bv_y)+0.25\,\mathrm{sinc}(bv_y-1)+0.25\,\mathrm{sinc}(bv_y+1)]. \tag{66}$$

d) BLACKMAN'S distribution. Let us accept that the amplitude distribution of the vibration velocity in the baffle S_0 is defined as follows (Fig. 5)

$$\varkappa(x_0, y_0) = \varkappa_0 \varkappa(x_0)\varkappa(y_0), \tag{67}$$

where

$$\varkappa(x_0) = \begin{cases} 0.42+0.5\cos(2\pi x_0/a)+0.08\cos(4\pi x_0/a) & \text{for } |x_0| \leqslant a/2, \\ 0 & \text{for } |x_0| > a/2 \end{cases} \tag{68}$$

and

$$\varkappa(y_0) = \begin{cases} 0.42+0.5\cos(2\pi y_0/b)+0.08\cos(4\pi y_0/b) & \text{for } |y_0| \leqslant b/2, \\ 0 & \text{for } |y_0| > b/2. \end{cases} \tag{69}$$

The mean square value of the distribution is equal to

$$D^2 = 0.093\varkappa_0^2 ab, \tag{70}$$

while its spatial spectrum (Fig. 5) is given as

$$K(v_x, v_y) = \varkappa_0 K(v_x)K(v_y), \tag{71}$$

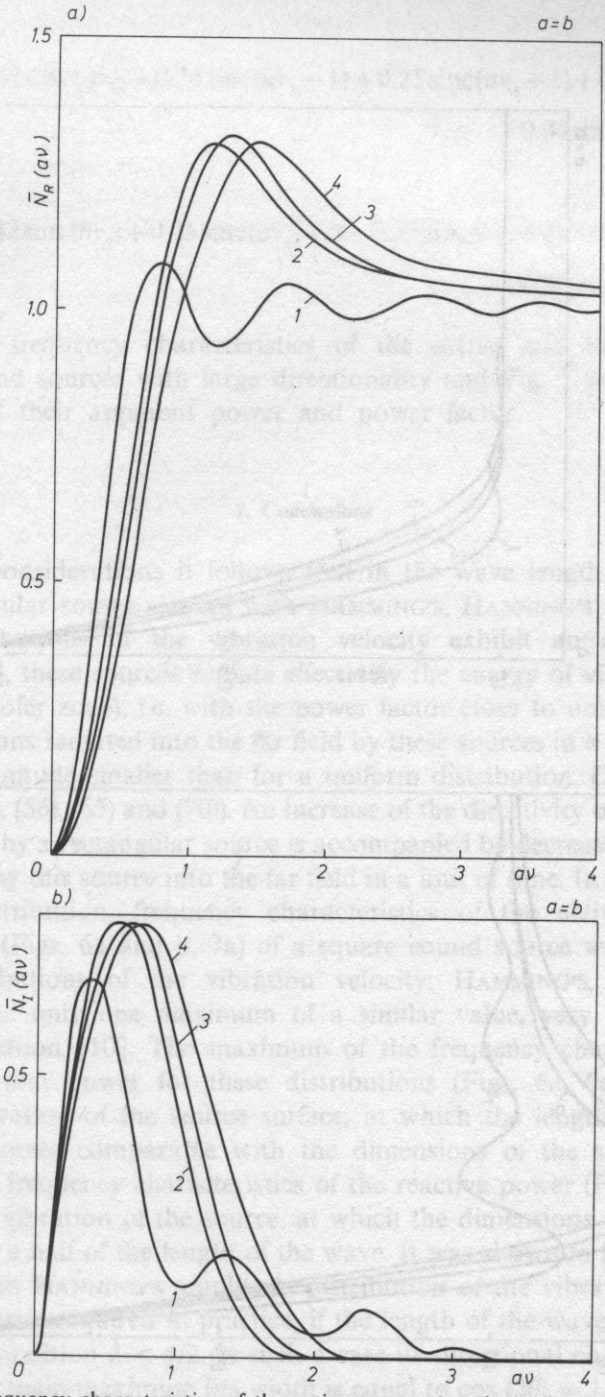

Fig. 6. Normalized frequency characteristics of the active power a) and reactive power b) of a square sound source with the following distributions: 1 — uniform, 2 — HAMMING'S, 3 — HANNING'S, 4 — BLACKMAN'S

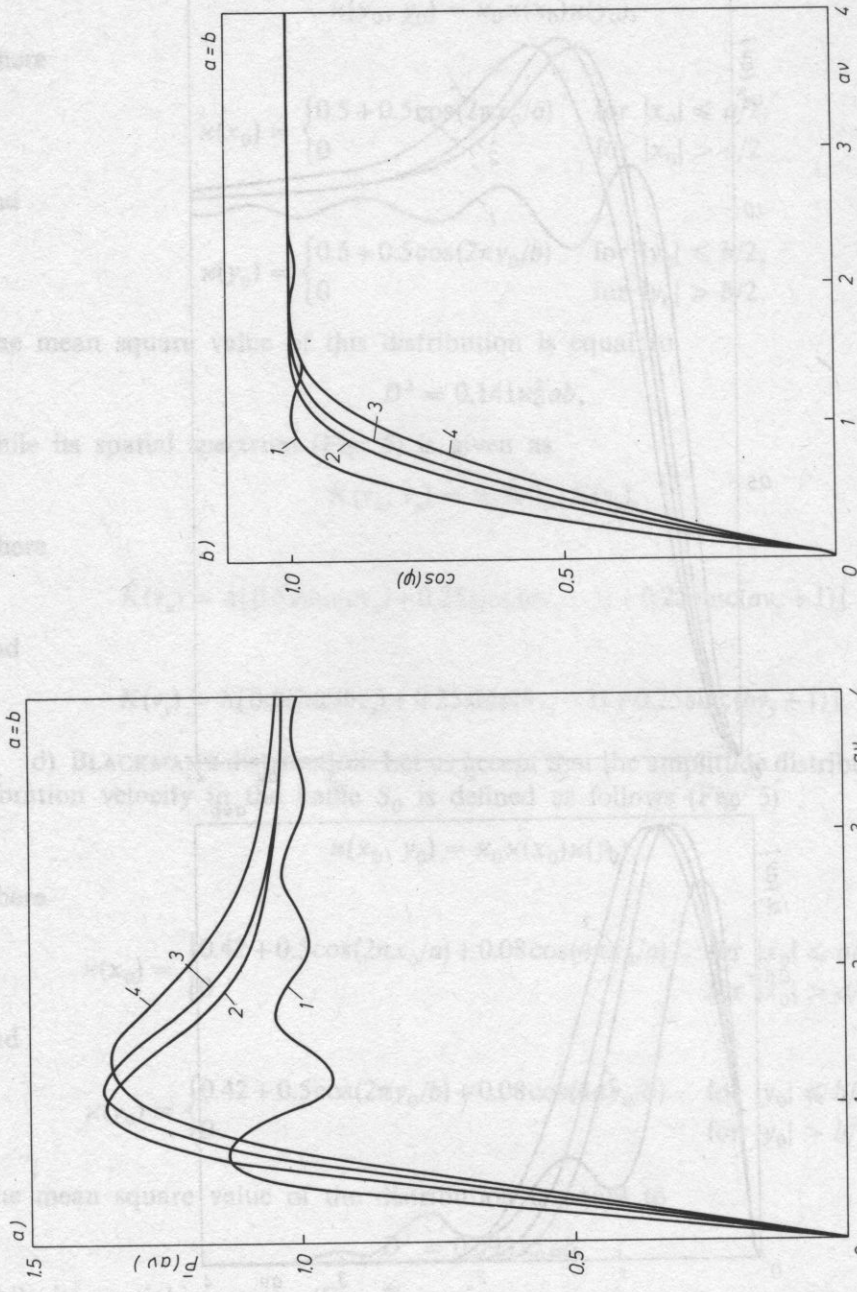

Fig. 7. Normalized frequency characteristics of the apparent power a) and the power factor b) of a square sound source with the following distributions: 1 — uniform, 2 — HAMMING'S, 3 — HANNING'S, 4 — BLACKMAN'S

where

$$K(v_x) = a[0.42\,\mathrm{sinc}(av_x) + 0.25\,\mathrm{sinc}(av_x - 1) + 0.25\,\mathrm{sinc}(av_x + 1) + 0.04\,\mathrm{sinc}(av_x - 2) + 0.04\,\mathrm{sinc}(av_x + 2)] \quad (72)$$

and

$$K(v_y) = b[0.42\,\mathrm{sinc}(bv_y) + 0.25\,\mathrm{sinc}(bv_y - 1) + 0.25\,\mathrm{sinc}(bv_y + 1) + 0.04\,\mathrm{sinc}(bv_y - 2) + 0.04\,\mathrm{sinc}(bv_y + 2)]. \quad (73)$$

Fig. 6 presents frequency characteristics of the active and reactive power of investigated sound sources with large directionality and Fig. 7 presents frequency characteristics of their apparent power and power factor.

7. Conclusions

From our considerations it follows that in the wave length range, in which analysed rectangular sound sources with HAMMING'S, HANNING'S and BLACKMAN'S amplitude distributions of the vibration velocity exhibit an adequately large directionality [5], these sources radiate effectively the energy of vibrations into the far field (Fraunhofer zone), i.e. with the power factor close to unity. However, the energy of vibrations radiated into the far field by these sources in a unit of time is by an order of magnitude smaller than for a uniform distribution. (This results from relationships (48), (56), (65) and (70)). An increase of the directivity of radiation of the vibration energy by a rectangular source is accompanied by decrease of the vibration energy radiated by this source into the far field in a unit of time. In comparison with the uniform distribution, frequency characteristics of the active, reactive and apparent power (Figs. 6a and b, 7a) of a square sound source with the following amplitude distributions of the vibration velocity: HAMMING'S, HANNING'S and BLACKMAN'S have only one maximum of a similar value, very much like for a Gaussian distribution [10]. The maximum of the frequency characteristic of the active and apparent power for these distributions (Figs. 6a, 7a) occurs at the frequency of vibration of the source surface, at which the length of the radiated sound wave becomes comparable with the dimensions of the source; while the maximum of the frequency characteristics of the reactive power (Fig. 6b) occurs at the frequency of vibration of the source, at which the dimensions of the source are comparable with a half of the length of the wave. It was shown in [5] that a square sound source with HANNING'S amplitude distribution of the vibration velocity has directivity properties required in practice, if the length of the wave radiated by this source satisfies condition $\lambda < a/2$. Is such a case its directional characteristic has a relatively narrow main maximum (its width is equal to $\cos(2\theta) = 1.4\,\lambda/a$ at the level of -3 dB) and sufficiently strongly damped ($\geqslant 32$ dB) and quickly decreasing (60

dB/decade) side maxima. At wave length $\lambda < a/2$ this source radiates its whole energy into the far field (Fig. 7b).

The method of determining energetic characteristics of plane sound sources, which was presented in this paper, can be applied in the estimation of energetic properties of various real plane sound sources on the basis of experimentally determined directional characteristics. It can be proved that the directional characteristic of a sound source is a fragment of the spatial spectrum of the amplitude distribution of the vibration velocity, produced by a given source in the baffle. A detailed analysis of this problem is presented in paper [5]. Measurements of the level of the directional characteristics of a sound source at a given spatial frequency v can be used for the calculation of its active power (26) with a chosen method of numerical integration. The frequency characteristic of the active power of an investigated sound source in the interesting to us range of spatial frequency v can be achieved by repeating these calculations for following spatial frequencies. In turn, on this basis the frequency characteristic of the reactive power of this source (42) can be calculated with the application of a chosen algorithm of a discrete Fourier transform. The sampling interval of the frequency characteristic of the active power and the truncate function of this characteristic has to be adequately chosen. These problems have been analysed in detail in papers [3] and [4].

The basic advantage of this method of determining energetic characteristics of sound sources is the possibility of its application in investigations of energetic properties of sources and systems of sound sources with arbitrary shape and arbitrary amplitude distribution of the vibration velocity on their surface. The simplicity and speed of obtaining neccessary results with the application of a computer is another advantage.

The limited applicability of this method is the disadvantage of this method. Namely — it can be used in investigations of energetic properties of plane sources and systems of sound sources situated in a baffle.

References

[1] W. T. CATHEY, *Optical information processing and holography*, John Wiley and Sons, New York 1974.

[2] L. E. KINSLER, A. R. FREY, A. B. COOPENS, J. V. SANDERS, *Fundamentals of acoustics*, John Wiley and Sons, New York 1982.

[3] A. V. OPPENHEIM, R. W. SCHAFER, *Digital signal processing*, Prentice-Hall Inc., New Jersey 1975.

[4] A. PUCH, *Nummerical methods of function spectral analysis*, WSP, Rzeszów 1984 (in Polish).

[5] A. PUCH, Rectangular source and systems of sound sources with large directionality, Archives of Acoustics, **10**, 1, 17–35 (1985).

[6] W. RDZANEK, *Integral formulas for the acoustic impedance of a plane source vibrating in an acoustically rigid plane baffle*, Archiwum Akustyki, **8**, 3, 283–291 (1973) (in Polish).

[7] W. RDZANEK, *Mutual and total acoustic impedance of a system of sound sources with a variable surface distribution of the vibration velocity*, WSP, Zielona Góra 1979 (in Polish).

[8] P. R. STEPANISHEN, *The radiation impedance of rectangular piston*, Journ. Sound Vib., **55**, 2, 275–288 (1977).

[9] R. WYRZYKOWSKI, Cz. SOŁTYS, *Calculation of the acoustic impedance of sound sources with known directivity*, Archiwum Akustyki, **7**, 3–4, 327–336 (1972) (in Polish).

[10] R. WYRZYKOWSKI, Cz. SOŁTYS, *Properties of a source with a Gaussian amplitude distribution of the vibration velocity*, Archivum Akustyki, **8**, 1, 81–89 (1973) (in Polish).

[11] J. SZABATIN, *Fundamentals of the theory of signals*, WKŁ, Warszawa 1982 (in Polish).

[12] A. WOJTKIEWICZ, *Elements of synthesis of digital filters*, WNT, Warszawa 1984 (in Polish).

Received on July 30, 1985; revised version on July 25, 1986.

THE NOISE-CON 87

"High Technology for Noise Control" was the theme of NOISE-CON 87, the 1987 National Conference on Noise Control Engineering. One hundred and twenty-five papers on technical topics on noise control engineering were presented at the three-day meeting which was held on the campus of The Pennsylvania State University in State College, Pennsylvania on 1987 June 8–10. Professor Jiri TICHY, Head of the Graduate Program in Acoustics at Penn State, was the General Chairman for the conference.

NOISE-CON 87 was sponsored jointly by the Penn State Graduate Program in Acoustics and the Institute of Noise Control Engineering (INCE). It was the eighth in a series of national conferences on noise control engineering which have been sponsored by INCE since 1973.

Subjects covered at the three-day meeting included noise emitted by gears, valves and steam tubes, axial and centrifugal fan noise, drill noise, chain saw noise, combustion noise, noise barriers, highway noise, sound absorptive materials, active noise cancellation, noise control of ships, and sound intensity techniques.

The papers presented at the conference have been collected into an 800-page bound volume which will be of interest to engineers concerned with noise control technology, government workers, consultants, educators and other individuals concerned with noise control technology.